

CHAPTER 1

ANISOTROPIC AND HETEROGENEOUS POLYMERIZED MEMBRANES

Leo Radzihovsky

Department of Physics, University of Colorado, Boulder, CO 80309

E-mail: radzihov@colorado.edu

In these lectures I describe long scale properties of fluctuating polymerized membranes in the presence of network anisotropy and random heterogeneities. Amazingly, even infinitesimal amount of these seemingly innocuous but physically important ingredients in the membrane's internal structure leads to a wealth of striking qualitatively new phenomena. Anisotropy leads to a “tubule” phase that is intermediate in its properties and location on the phase diagram between previously discussed “crumpled” and “flat” phases. At low temperature, network heterogeneity generates conformationally glassy phases, with membrane normals exhibiting glass order analogous to spin-glasses. The common thread to these distinct membrane phases is that they exhibit universal anomalous elasticity, (singularly length-scale dependent elastic moduli, universal Poisson ratio, etc.), driven by thermal fluctuations and/or disorder and controlled by a nontrivial low-temperature fixed point.

1. Preamble

The nature of a membrane's in-plane order, with three well-studied universality classes, the isotropic liquid¹, hexatic liquid² and solid³, crucially affects its conformational properties. The most striking illustration of this (discussed in lectures by Yacov Kantor and by David Nelson) is the stabilization in polymerized membranes (but not fluid ones, that are always crumpled¹ beyond a persistence length⁴) of a “flat” phase³, with long-range orientational order in the local membrane normals^{5,6}, that is favored at low temperature over the entropically preferred high-temperature crumpled state. In a beautiful “order from disorder” phenomenon, a subtle interplay of wild thermal fluctuations with nonlinear membrane elasticity (made possible by a finite shear modulus of a solid) infinitely enhances membrane's bending rigidity, thereby stabilizing the flat phase against these very fluctuations.³ A universal fluctuation-driven “anomalous elasticity” characterizes the resulting flat phase, with length-scale dependent elastic moduli, non-Hookean stress-strain relation, and a universal negative Poisson ratio.^{7,8,9}

Given such qualitative distinction between liquid and solid membranes, it is perhaps not too surprising that other in-plane orders can have important qualitative

effects on membrane's long-scale properties. In these lectures I will discuss two such ingredients, namely, membrane network in-plane *anisotropy* (Section 2) and *heterogeneity* (Section 3) in fluctuating *polymerized* membranes, and will show that these seemingly innocuous generalizations, indeed lead to a wealth of new phenomena that are the subject of these lectures.

2. Anisotropic Polymerized Membranes

2.1. Motivation and introduction

In addition to the basic theoretical motivation, the interest in anisotropic polymerized membranes is naturally driven by a number of possible experimental realizations, some of which are illustrated in Fig.1. One example is a tethered membrane

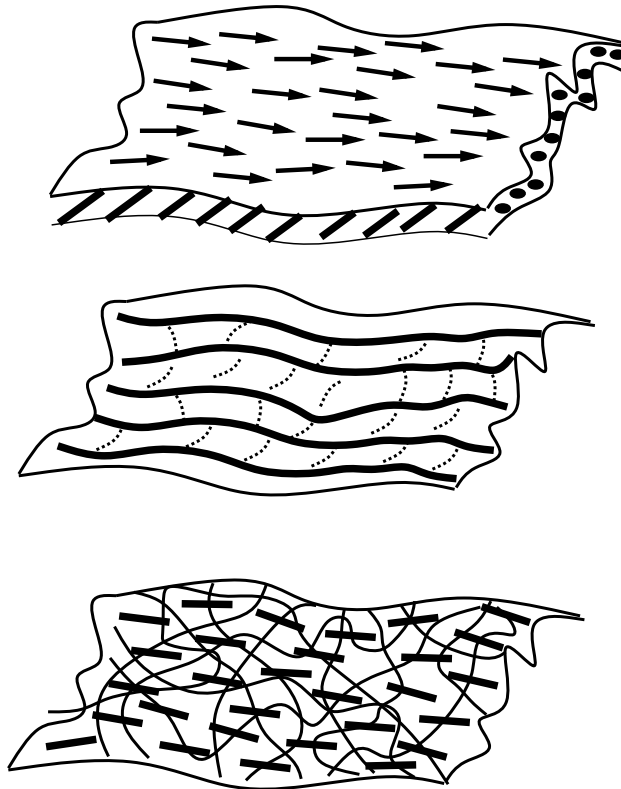


Fig. 1. Examples of anisotropic polymerized membranes with (a) a polymerized-in lipid tilt order in a bilayer membrane, (b) a weakly crosslinked array of linear polymers, and (c) a spontaneous in-plane nematic order in a nematic elastomer membrane.

made through photo-polymerization of a fluid phospholipid membrane exhibiting

lipid tilt order. On average the lipids are tilted relative to the membrane normal, inducing a vector in-plane order and an intrinsic elastic anisotropy that can in principle be aligned with an electric or a magnetic field and polymerized in. Another possible method¹⁰ of fabricating polymerized sheets is by cross-linking a stretched out, aligned array of linear polymers, that would clearly lead to an intrinsically anisotropic tethered membrane. One other promising candidate is a two-dimensional sheet of a nematic elastomer¹¹, a material that received considerable attention recently because of its novel elastic and electro-optic properties.¹² These cross-linked liquid-crystal polymer gels exhibit all standard liquid-crystal phases and therefore in their nematic state are highly anisotropic.

Almost 10 years ago, it was discovered¹³ that in-plane anisotropy has a dramatic qualitative effect on the global phase diagram of polymerized membranes. As illustrated in Fig.2, it leads to an entirely new “tubule” phase of a polymerized membrane (see Fig.3), that is crumpled along one and extended along the other of the two membrane axes, with wild undulations about its average cylindrical geometry.¹⁴

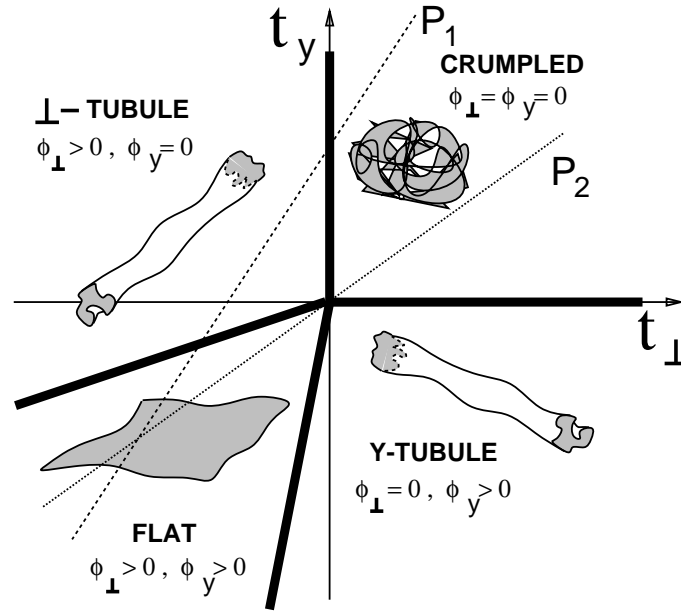


Fig. 2. Phase diagram for anisotropic tethered membranes showing crumpled, tubule and flat phases as a function of reduced temperatures $t_{\perp} \propto T - T_c^{\perp}$, $t_y \propto T - T_c^y$.

This is possible because in an anisotropic membrane, where symmetry between x_{\perp} and y axes is broken, (e.g., curvature moduli $\kappa_{x_{\perp}} \neq \kappa_y$) the x_{\perp} - and y -directed tangents $\vec{\zeta}_{\perp} = \partial_{\perp} \vec{r}$ and $\vec{\zeta}_y = \partial_y \vec{r}$ will generically order at two distinct temperatures $T_c^{\perp} \sim \kappa_{x_{\perp}}$ and $T_c^y \sim \kappa_y$, respectively, thereby allowing two intermediate tubule

states: (1) x_{\perp} -extended tubule with $\langle \vec{\zeta}_{\perp} \rangle \neq 0$, $\langle \vec{\zeta}_y \rangle = 0$, for $T_c^y < T < T_c^{\perp}$ and (2) y -extended tubule with $\langle \vec{\zeta}_{\perp} \rangle = 0$, $\langle \vec{\zeta}_y \rangle \neq 0$, for $T_c^{\perp} < T < T_c^y$.

The direct crumpling transition occurs in such more generic anisotropic membrane only for that special set of cuts through the phase diagram (like P_2) that pass through the origin and is in fact tetra-critical. Generic paths (like P_1) will experience *two* phase transitions, crumpled-to-tubule, and tubule-to-flat, that are in distinct universality classes. The tubule phase is therefore not only generically possible, but actually unavoidable, in membranes with any type or amount of *intrinsic anisotropy*.¹⁸

As illustrated in Fig.3 the tubule is characterized by its thickness R_G , (the radius of gyration of its crumpled boundary), and its undulations h_{rms} transverse to its average axis of orientation. Quite generally, (for a y -extended tubule of an $L_{\perp} \times L_y$ membrane) they obey the scaling laws:

$$R_G(L_{\perp}, L_y) = L_{\perp}^{\nu} S_R(L_y/L_{\perp}^z), \quad h_{rms}(L_{\perp}, L_y) = L_y^{\zeta} S_h(L_y/L_{\perp}^z), \quad (1)$$

where the roughness exponent $\zeta = \nu/z$, and the anisotropy exponent $z = (1 + 2\nu)/(3 - \eta_{\kappa}) < 1$ are expressed in terms two independent universal exponents: the radius of gyration exponent $\nu < 1$ and the anomalous elasticity exponent η_{κ} for the tubule bending rigidity defined by $\kappa \sim L_y^{\eta_{\kappa}}$. The *universal* scaling functions $S_{R,h}(x)$

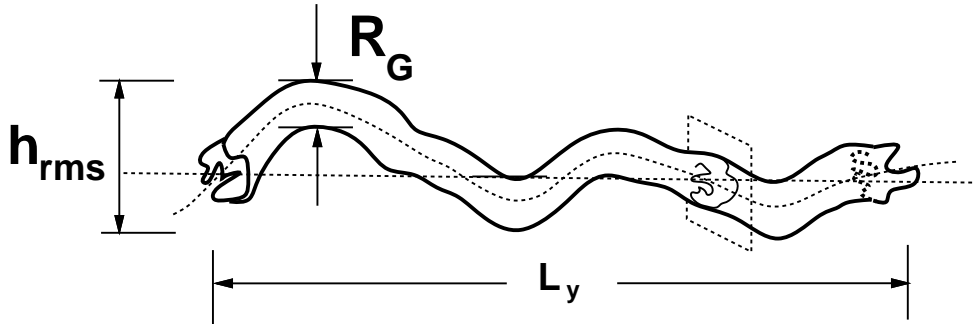


Fig. 3. Schematic of the y -tubule phase of anisotropic polymerized membrane, with thickness R_G and roughness h_{rms} .

have the limiting forms:

$$S_R(x) \propto \begin{cases} x^{\zeta - \nu_p/z}, & \text{for } x \rightarrow 0 \\ \text{constant}, & \text{for } x \rightarrow \infty \end{cases} \quad (2)$$

$$S_h(x) \propto \begin{cases} \text{constant}, & \text{for } x \rightarrow 0 \\ x^{\frac{3}{2} - \zeta}, & \text{for } x \rightarrow \infty \end{cases}, \quad (3)$$

where ν_p is the radius of gyration exponent of a coiled linear polymer $\approx 3/5$. These asymptotic forms emerge from general requirements (supported by detailed renormalization group calculations¹³) that in the limit of a very thin tubule (in the curled

up \perp direction) the tubule's height undulations $h_{rms}(L_y)$ reproduce statistics of a linear polymer of length L_y and width L_\perp . And, that in the opposite limit of vanishing L_y , scaling functions must recover the radius of gyration $R_G(L_\perp) \sim L_\perp^{\nu_p}$ of a linear polymer of length L_\perp and thickness L_y .

The scaling forms, Eq.2 and 3 imply that for a "roughly square" membrane – that is, one with $L_\perp \sim L_y \equiv L$ – in the limit $L \rightarrow \infty$

$$R_G(L_\perp \sim L_y \equiv L) \propto L^\nu, \quad h_{rms}(L_\perp \sim L_y \equiv L) \propto L^{1-\eta_\kappa z/2}. \quad (4)$$

Combining this with detailed renormalization group calculations, that find a strictly positive η_κ ,¹³ shows that $h_{rms} \ll L$ for a large roughly square membrane. Thus, the end-to-end orientational fluctuations $\theta \sim h_{rms}/L \propto L^{-\eta_\kappa/2} \rightarrow 0$ as $L \rightarrow \infty$ for such a roughly square membrane, proving that tubule order (which requires orientational persistence in the extended direction) is stable against undulations of the tubule embedded in $d = 3$ dimensions.

The rest of Section 2 is devoted to developing a model of an anisotropic polymerized membrane and using it to study phase transitions into and out of the tubule phase and the anomalous elastic properties of a fluctuating tubule summarized above.

2.2. Model

A model for anisotropic membranes is a generalization of the isotropic model discussed in David Nelson's lectures.⁶ As there, we characterize the configuration of the membrane by the position $\vec{r}(\mathbf{x})$ in the d -dimensional embedding space of the point in the membrane labeled by a D -dimensional internal co-ordinate \mathbf{x} , with $d = 3$ and $D = 2$ corresponding to the physical case of interest.

Rotational and translational symmetries require that the Landau-Ginzburg free energy F is an expansion in powers of tangent vectors $\vec{\xi}_{\perp,y} = \partial_{\perp,y} \vec{r}$ and their gradients

$$\begin{aligned} F[\vec{r}(\mathbf{x})] = & \frac{1}{2} \int d^{D-1} x_\perp dy \left[\kappa_\perp (\partial_\perp^2 \vec{r})^2 + \kappa_y (\partial_y^2 \vec{r})^2 + \kappa_{\perp y} \partial_y^2 \vec{r} \cdot \partial_\perp^2 \vec{r} \right. \\ & + t_\perp (\partial_\alpha^\perp \vec{r})^2 + t_y (\partial_y \vec{r})^2 + \frac{u_{\perp\perp}}{2} (\partial_\alpha^\perp \vec{r} \cdot \partial_\beta^\perp \vec{r})^2 + \frac{u_{yy}}{2} (\partial_y \vec{r} \cdot \partial_y \vec{r})^2 + u_{\perp y} (\partial_\alpha^\perp \vec{r} \cdot \partial_y \vec{r})^2 \\ & \left. + \frac{v_{\perp\perp}}{2} (\partial_\alpha^\perp \vec{r} \cdot \partial_\alpha^\perp \vec{r})^2 + v_{\perp y} (\partial_\alpha^\perp \vec{r})^2 (\partial_y \vec{r})^2 \right] + \frac{b}{2} \int d^D x \int d^D x' \delta^{(d)}(\vec{r}(\mathbf{x}) - \vec{r}(\mathbf{x}')), \end{aligned} \quad (5)$$

where we have taken the membrane to be isotropic in the $D - 1$ membrane directions \mathbf{x}_\perp , orthogonal to one special direction, y . While at first glance F might appear quite formidable, in fact (aside from the last term), in terms of the tangent order parameter $\vec{\xi}_{\perp,y}$ it has a standard form of the Landau's ϕ^4 theory. The first three terms in F (the κ terms) represent the anisotropic bending energy of the membrane. The elastic constants t_\perp and t_y are the most strongly temperature dependent

parameters in the model, changing sign from large, positive values at high temperatures to negative values at low temperatures. The u and v quartic elastic terms are needed to stabilize the membrane when one or both of the elastic constants t_{\perp} , t_y become negative. The final, b term in Eq.5 represents the self-avoidance of the membranes, i.e., its steric or excluded volume interaction.

2.3. Mean-field theory

In mean-field theory, we seek a configuration $\vec{r}(\mathbf{x})$ that minimizes the free energy, Eq.5. The curvature energies $\kappa_{\perp} (\partial_{\perp}^2 \vec{r})^2$ and $\kappa_y (\partial_y^2 \vec{r})^2$ are clearly minimized when $\vec{r}(\mathbf{x})$ is linear in \mathbf{x}

$$\vec{r}(\mathbf{x}) = (\zeta_{\perp} \mathbf{x}_{\perp}, \zeta_y y, 0, 0, \dots, 0) . \quad (6)$$

Inserting Eq.6 into Eq.5, and for now neglecting the self-avoidance, we obtain the mean-field free energy density for anisotropic membranes

$$f_{\text{mft}} = \frac{1}{2} [t_y \zeta_y^2 + t_{\perp} (D-1) \zeta_{\perp}^2 + \frac{1}{2} u'_{\perp\perp} (D-1)^2 \zeta_{\perp}^4 + \frac{1}{2} u_{yy} \zeta_y^4 + v_{\perp y} (D-1) \zeta_{\perp}^2 \zeta_y^2] , \quad (7)$$

Minimizing the free energy over order parameters ζ_{\perp} and ζ_y yields two possible phase diagram topologies, depending on whether $u'_{\perp\perp} u_{yy} > v_{\perp y}^2$ or $u'_{\perp\perp} u_{yy} < v_{\perp y}^2$.¹⁹

For $u'_{\perp\perp} u_{yy} > v_{\perp y}^2$, the phase diagram is given in Fig.2. For $t_{\perp} > 0$ and $t_y > 0$, average tangent vectors ζ_{\perp} and ζ_y both vanish, describing a crumpled (collapsed to the origin) membrane.

In the regime between the positive t_{\perp} -axis and the $t_y < 0$ part of the $t_y = (u_{yy}/v_{\perp y})t_{\perp}$ line, lies the y -tubule phase, characterized by $\zeta_{\perp} = 0$ and $\zeta_y = \sqrt{|t_y|/u_{yy}} > 0$: the membrane is extended in the y -direction but crumpled in all $D-1$ \perp -directions.

The \perp -tubule phase is the analogous phase with the y and \perp directions reversed, $\zeta_y = 0$ and $\zeta_{\perp} = \sqrt{|t_{\perp}|/u_{\perp\perp}} > 0$, and lies between the $t_{\perp} < 0$ segment of the line $t_y = (v_{\perp y}/u'_{\perp\perp})t_{\perp}$ and the positive t_y axis.

Finally, the flat phase, characterized by both

$$\zeta_{\perp} = [(|t_{\perp}|u_{yy} - |t_y|v_{\perp y})/(u'_{\perp\perp}u_{yy} - v_{\perp y}^2)]^{1/2} > 0 , \quad (8)$$

$$\zeta_y = [(|t_y|u_{\perp\perp} - |t_{\perp}|v_{\perp y})/(u'_{\perp\perp}u_{yy} - v_{\perp y}^2)]^{1/2} > 0 , \quad (9)$$

lies between the $t_{\perp} < 0$ segment of the line $t_y = (u_{yy}/v_{\perp y})t_{\perp}$ and the $t_y < 0$ segment of the line $t_y = (v_{\perp y}/u'_{\perp\perp})t_{\perp}$.

For $u'_{\perp\perp} u_{yy} < v_{\perp y}^2$, the flat phase disappears, and is replaced by a direct first-order transition from \perp -tubule to y -tubule along the locus $t_y = (v_{\perp y}/u'_{\perp\perp})t_{\perp}$ (see Fig.4) . The boundaries between the tubule and the crumpled phases remain the positive t_y and t_{\perp} axes, as for $u'_{\perp\perp} u_{yy} > v_{\perp y}^2$ case.

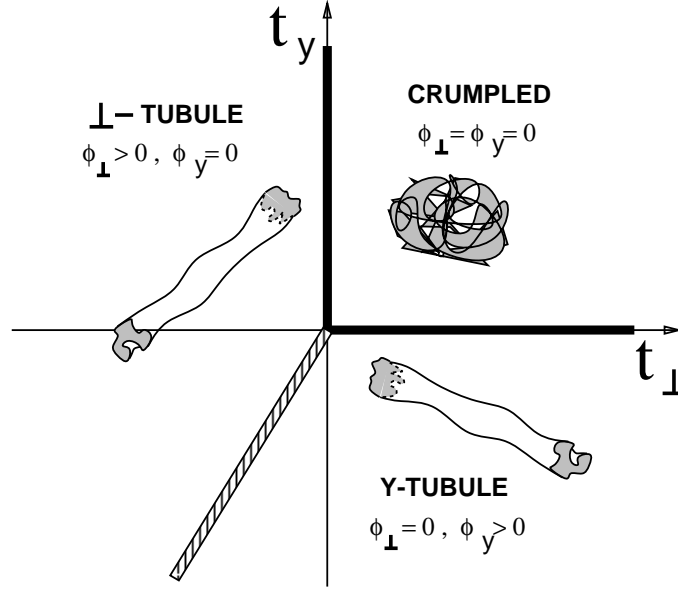


Fig. 4. Phase diagram for anisotropic tethered membranes showing a new tubule phase, for the range of elastic parameters when the intermediate flat phase disappears. A first-order phase transition separates y - and \perp -tubule phases.

2.4. Fluctuations and self-avoidance in the crumpled and flat phases

Although anisotropy has dramatic effects on the phase diagram of polymerized membranes, it does not modify the nature of the crumpled and flat phases.²⁰ To see this for the crumpled phase note that when both t_{\perp} and t_y are positive, all of the other local terms in Eq.5, i.e., the κ , u , and v -terms, are subdominant at long wavelengths. When these irrelevant terms are neglected, a simple change of variables $\mathbf{x}_{\perp} = \mathbf{x}'\sqrt{t_{\perp}/t_y}$ makes the remaining energy isotropic. Thus, the entire crumpled phase is identical in its scaling properties to that of isotropic membranes. In particular, the membrane in this phase has a radius of gyration $R_G(L)$ which scales with membrane linear dimension L like L^{ν} , with $\nu = (D+2)/(d+2)$ in Flory theory, and very similar values predicted by ϵ -expansion techniques.^{22,23,24}

Fluctuations in the flat phase can be incorporated by considering small deviations from the mean-field conformation in Eq.6

$$\vec{r}(\mathbf{x}) = \left(\zeta_{\perp} \mathbf{x}_{\perp} + u_{\perp}(\mathbf{x}), \zeta_y y + u_y(\mathbf{x}), \vec{h}(\mathbf{x}) \right), \quad (10)$$

where $u_{\alpha}(\mathbf{x})$ are D in-plane phonon fields and $h_i(\mathbf{x})$ are $d_c = d - D$ out-of-plane height undulation fields. Inserting this into free energy, Eq.5, with t_{\perp} and t_y both in the range in which the flat phase is stable, we obtain the uniaxial elastic energy studied by Toner.²⁵ As he showed, amazingly, fluctuation renormalize this anisotropic

elastic energy into the *isotropic* membrane elastic energy studied previously.^{3,7,8,9} Therefore, in the flat phase, and at sufficiently long scales, the anisotropic membranes behave exactly like isotropic ones.

2.4.1. Anomalous elasticity of the flat phase

This in particular implies that the flat phase of anisotropic membranes is stable against thermal fluctuations even though it breaks continuous (rotational) symmetry and is two-dimensional.²⁶ As in isotropic membranes, this is due to the fact that at long wavelengths these very thermal fluctuations drive the effective (renormalized) bend modulus κ to infinity^{3,7,8,9}, thereby suppressing effects of these same fluctuations that seek to destabilize the flat phase, resulting in an Esher-like “order-from-disorder” phenomenon.

Specifically, $\kappa(q)$ becomes wavevector dependent, and diverges like $q^{-\eta_\kappa}$ as $q \rightarrow 0$. In the flat phase the standard Lamé coefficients μ and λ ²⁷ are also infinitely renormalized and become wavevector dependent, vanishing in the $q \rightarrow 0$ limit as $\mu(q) \sim \lambda(q) \sim q^{\eta_u}$. The flat phase is furthermore novel in that it is characterized by a universal *negative* Poisson ratio^{7,9} which for $D = 2$ is defined as the long wavelength limit $q \rightarrow 0$ of $\sigma = \lambda(q)/(2\mu(q) + \lambda(q))$. The transverse undulations in the flat phase, i.e. the membrane roughness h_{rms} scales with the internal size of the membrane as $h_{rms} \sim L^\zeta$, with $\zeta = (4 - D - \eta_\kappa)/2$, exactly. Furthermore, an underlying rotational invariance imposes an exact Ward identity between η_κ and η_u , $\eta_u + 2\eta_\kappa = 4 - D$. This leaves only a single independent exponent, characterizing the properties of the flat phase of even anisotropic membranes.

To appreciate how exotic and unusual this anomalous elasticity really is one only needs to observe that most ordered and disordered states of matter (systems with quenched disorder being prominent exceptions²⁸), are in a sense trivial, with fluctuations about them described by a harmonic theory controlled by a Gaussian fixed point.²⁹ That is, generically, qualitatively important effects of fluctuations are confined to the vicinity of isolated critical points, where a system is tuned to be “soft”, and characterized by low energy excitations. However, there exists a novel class of systems, with flat phase of polymerized membranes as a prominent member (that also includes smectic^{30,31} and columnar liquid crystals³², vortex lattices in putative magnetic superconductors³³, and nematic elastomers^{12,34,35,36,37,38}) whose ordered states are a striking exception to this rule. A unifying feature of these phases is their underlying, spontaneously broken rotational invariance, that strictly enforces a particular “softness” of the corresponding Goldstone mode Hamiltonian. As a consequence, the usually small nonlinear elastic terms are in fact comparable to harmonic ones, and therefore must be taken into account. Similarly to their effects near continuous phase transitions (where they induce universal power-law anomalies), but extending throughout an ordered phase, fluctuations drive nonlinearities to qualitatively modify such soft states. The resulting strongly interacting ordered states at long scales exhibit rich phenomenology such as a universal nonlo-

cal elasticity, a strictly nonlinear response to an arbitrarily weak perturbation and a universal ratio of wavevector-dependent singular elastic moduli, all controlled by a nontrivial infrared stable fixed point illustrated in Fig.5.

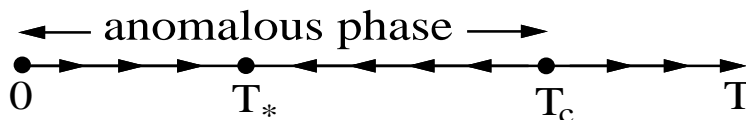


Fig. 5. Renormalization group flow for anomalously elastic solids, with T_c the transition temperature to the ordered state and T_* a nontrivial infrared stable fixed point controlling properties of the strongly interacting ordered, critical-like state.

2.4.2. SCSA of the flat phase

The study of such anomalous elasticity in polymerized membranes was initiated by Nelson and Peliti using a simple one-loop self-consistent theory, that assumed a non-renormalization of the in-plane elastic Lamé' constants.³ They found that phonon-mediated interaction between capillary waves leads to a divergent bending rigidity with $\eta_\kappa = 1$ and membrane roughness exponent $\zeta = 1/2$. Subsequent controlled $\epsilon = 4 - D$ and $1/d_c$ expansions^{7,8} confirmed existence of anomalous elasticity, and discovered an additional effect of softening (screening) of in-plane elasticity by out-of-plane undulations, that lead to a vanishing of long-scale Lamé' coefficients $\lambda(q) \sim \mu(q) \sim q^{\eta_u}$.

Here we treat anomalous elasticity within the so-called self-consistent screening approximation (SCSA), first applied to the study of the flat phase of polymerized membranes by Le Doussal and Radzihovsky⁹. The attractive feature of SCSA is that it becomes exact in three complementary limits. By construction, it is exact in the large embedding dimension $d_c \rightarrow \infty$ limit and agrees with the systematic $1/d$ analysis of Gutter, et al.⁸ Because of Ward identities associated with rotational invariance it is exact (at any d) to lowest order $\epsilon = 4 - D$, i.e., agrees with one-loop results of Aronovitz and Lubensky.⁷ (It would be very interesting to check predictions of SCSA to order ϵ^2 , however technical difficulties with two-loop calculations have so far precluded this³⁹). And finally it gives exact value of $\eta_\kappa(D)$ for $d_c = 0$. Given these exact constraints, it is not surprising that for physical dimensions ($D = 2, d = 3$) SCSA exponents and the universal negative Poisson ratio⁹ compare so well with latest, largest scale numerical simulations, discussed in lectures by Mark Bowick.⁴⁰

As discussed above, at sufficiently long scales, flat phase of an anisotropic polymerized membrane is identical to that of an isotropic one²⁵, and is described by an isotropic effective free energy that is a sum of a bending and an in-plane elastic

energies:

$$F[\vec{h}, \mathbf{u}] = \int d^D x \left[\frac{\kappa}{2} (\nabla^2 \vec{h})^2 + \mu u_{\alpha\beta}^2 + \frac{\lambda}{2} u_{\alpha\alpha}^2 \right], \quad (11)$$

where the strain tensor is $u_{\alpha\beta} = \frac{1}{2}(\partial_\alpha u_\beta + \partial_\beta u_\alpha + \partial_\alpha \vec{h} \cdot \partial_\beta \vec{h})$. To implement the SCSA in the flat phase it is convenient to first integrate out the noncritical phonons fields u_α obtaining a quartic theory for interacting Goldstone tangent vector modes $\partial_\alpha \vec{h}$, described by free energy

$$F[\vec{h}] = \int d^D x \left[\frac{\kappa}{2} (\nabla^2 \vec{h})^2 + \frac{1}{4d_c} (\partial_\alpha \vec{h} \cdot \partial_\beta \vec{h}) R_{\alpha\beta,\gamma\delta} (\partial_\gamma \vec{h} \cdot \partial_\delta \vec{h}) \right] \quad (12)$$

where for convenience, we rescaled Lamé coefficients so that the quartic coupling is of order $1/d_c$. The four-point coupling fourth-rank tensor is given by

$$R_{\alpha\beta,\gamma\delta} = \frac{K - 2\mu}{2(D-1)} P_{\alpha\beta}^T P_{\gamma\delta}^T + \frac{\mu}{2} (P_{\alpha\gamma}^T P_{\beta\delta}^T + P_{\alpha\delta}^T P_{\beta\gamma}^T), \quad (13)$$

where $P_{\alpha\beta}^T = \delta_{\alpha\beta} - q_\alpha q_\beta / q^2$ is a transverse (to \mathbf{q}) projection operator. The convenience of this decomposition is that $K = 2\mu(2\mu + D\lambda)/(2\mu + \lambda)$ and μ moduli renormalize independently and multiplicatively.

To determine the renormalized elasticity, we set up a $1/d_c$ -expansion^{41,42,43} for 2-point and 4-point correlation functions of \vec{h} , and turn them into a closed self-consistent set of two coupled integral equations for self-energy $\Sigma(\mathbf{k})$ that define SCSA

$$\Sigma(\mathbf{k}) = \frac{2}{d_c} k_\alpha k_\beta k_\gamma k_\delta \int_q \tilde{R}_{\alpha\beta,\gamma\delta}(\mathbf{q}) G(\mathbf{k} - \mathbf{q}), \quad (14)$$

$$\tilde{R}_{\alpha\beta,\gamma\delta}(\mathbf{q}) = R_{\alpha\beta,\gamma\delta}(\mathbf{q}) - R_{\alpha\beta,\mu\nu}(\mathbf{q}) \Pi_{\mu\nu,\mu'\nu'}(\mathbf{q}) \tilde{R}_{\mu'\nu',\gamma\delta}(\mathbf{q}), \quad (15)$$

where $G(\mathbf{k}) \equiv 1/(\kappa k^4 + \Sigma(\mathbf{k})) \equiv 1/(\kappa(\mathbf{k})k^4)$ is the renormalized propagator, $R_{\alpha\beta,\gamma\delta}(\mathbf{q})$ the bare quartic interaction vertex and $\tilde{R}_{\alpha\beta,\gamma\delta}(\mathbf{q})$ the "screened" interaction vertex dressed by the vacuum polarization bubbles $\Pi_{\alpha\beta,\gamma\delta}(\mathbf{q}) = \int_p p_\alpha p_\beta p_\gamma p_\delta G(\mathbf{p}) G(\mathbf{q} - \mathbf{p})$, and tensor multiplication is defined above.

In the long wavelength limit these integral equations are solved exactly by a renormalized propagator $G(\mathbf{k}) \approx 1/\Sigma(\mathbf{k}) \approx Z/k^{4-\eta_\kappa}$, with Z a non-universal amplitude. Substituting this ansatz into Eqs.14,15 and solving for the renormalized elastic Lamé moduli, we find that indeed they must vanish as a universal power, with $\mu(\mathbf{q}) \propto \lambda(\mathbf{q}) \sim q^{\eta_u}$, and the phonon anomalous exponent $\eta_u = 4 - D - 2\eta_\kappa$ related to η_κ by dimensional analysis (power-counting on q) first obtained by Nelson and Peliti.³ This recovers the celebrated exponent relation enforced by the underlying rotational invariance of the membrane in the embedding space. The information about remaining independent exponent η_κ resides in the η_κ -dependent *amplitudes* of above equations. Cancelling out the nonuniversal scale Z , we obtain

$$d_c = \frac{2}{\eta_\kappa} D(D-1) \frac{\Gamma[1 + \frac{1}{2}\eta_\kappa] \Gamma[2 - \eta_\kappa] \Gamma[\eta_\kappa + D] \Gamma[2 - \frac{1}{2}\eta_\kappa]}{\Gamma[\frac{1}{2}D + \frac{1}{2}\eta_\kappa] \Gamma[2 - \eta_\kappa - \frac{1}{2}D] \Gamma[\eta_\kappa + \frac{1}{2}D] \Gamma[\frac{1}{2}D + 2 - \frac{1}{2}\eta_\kappa]}, \quad (16)$$

that determines $\eta_\kappa(D, d)$ within SCSA. For $D = 2$ this equation can be simplified, and one finds

$$\eta_\kappa(D = 2, d_c) = \frac{4}{d_c + \sqrt{16 - 2d_c + d_c^2}}. \quad (17)$$

Thus for physical membranes ($d_c = 1$) we obtain: $\eta_\kappa = 0.821$, $\eta_u = 0.358$ and:

$$\zeta = 1 - \frac{\eta_\kappa}{2} = \frac{\sqrt{15} - 1}{\sqrt{15} + 1} = 0.590. \quad (18)$$

At long length scales SCSA also gives a universal ratio between renormalized in-plane elastic moduli determined by $\tilde{R}_{\alpha\beta,\gamma\delta}(\mathbf{q})$, Eq.15, and therefore predicts a universal and *negative* Poisson ratio

$$\text{Lim}_{q \rightarrow 0} \sigma \equiv \frac{\lambda(q)}{2\mu(q) + (D-1)\lambda(q)} = -\frac{1}{3}. \quad (19)$$

that compares extremely well with the most recent and largest simulations.⁴⁰

Expanding the result Eq.16 in $1/d_c$ we obtain:

$$\eta_\kappa = \frac{8}{d_c} \frac{D-1}{D+2} \frac{\Gamma[D]}{\Gamma[\frac{D}{2}]^3 \Gamma[2 - \frac{D}{2}]} + O\left(\frac{1}{d_c^2}\right), \quad (20)$$

$$= \frac{2}{d_c} + O\left(\frac{1}{d_c^2}\right), \quad \text{for } D = 2, \quad (21)$$

which coincides with the exact result^{8,7}, as expected by construction of the SCSA. Similarly, expanding Eq.16 to first order in $\epsilon = 4 - D$ we find:

$$\eta_\kappa = \frac{\epsilon}{2 + d_c/12}, \quad (22)$$

also in agreement with the exact result.⁷ This is not, however, a general property of SCSA, but is special to membranes, and can be traced to the convergence of the vertex and box diagrams.

Because in the flat phase, widely intrinsically separated parts of the membranes (i.e., points \mathbf{x} and \mathbf{x}' , with $|\mathbf{x} - \mathbf{x}'|$ large) do not bump into each other (i.e., never have $\vec{r}(\mathbf{x}) = \vec{r}(\mathbf{x}')$), the self-avoidance interaction in Eq.5 is irrelevant in the flat phase. Hence we expect above predictions to accurately describe conformational properties of physical isotropic and anisotropic polymerized membranes.

2.5. Fluctuations in “phantom” tubules

Thermal fluctuations of the (y -) tubule about the mean-field state $\vec{r}_o(\mathbf{x}) = \zeta_y(y, \vec{0})$ are described by conformation,

$$\vec{r}(\mathbf{x}) = (\zeta_y y + u(\mathbf{x}), \vec{h}(\mathbf{x})), \quad (23)$$

where $\vec{h}(\mathbf{x})$ is a $d - 1$ -component vector field orthogonal to the tubule and $u(\mathbf{x})$ is a scalar phonon field along the tubule (taken along y -axis). The order parameter

ζ_y is a tubule extension scale that is slightly modified by thermal fluctuations from the mean-field value given in Sec.2.3 and is determined by the condition that all linear terms in $\vec{h}(\mathbf{x})$ and $u(\mathbf{x})$ in the renormalized elastic free energy exactly vanish. This criterion guarantees that $\vec{h}(\mathbf{x})$ and $u(\mathbf{x})$ represent fluctuations around the true tubule ground state.

Inserting the decomposition Eq.23 into the free energy Eq.5, neglecting irrelevant terms (e.g., phonon nonlinearities), and, for the moment ignoring the self-avoidance interaction, gives $F = F_{mft} + F_{el}$, where F_{mft} is given by Eq.7 (with $\zeta_{\perp} = 0$ and $F_{el}[u(\mathbf{x}), \vec{h}(\mathbf{x})]$ is the fluctuating elastic free energy part

$$F_{el} = \frac{1}{2} \int d^{D-1} x_{\perp} dy \left[\kappa (\partial_y^2 \vec{h})^2 + t (\partial_{\alpha}^{\perp} \vec{h})^2 + g_{\perp} (\partial_{\alpha}^{\perp} u)^2 + g_y (\partial_y u + \frac{1}{2} (\partial_y \vec{h})^2)^2 \right], \quad (24)$$

where $\kappa \equiv \kappa_y$, $t \equiv t_{\perp} + v_{\perp y} \zeta_y^2$, $g_y \equiv u_{yy} \zeta_y^2 / 2$, $g_{\perp} \equiv t + u_{\perp y} \zeta_y^2$, and $\gamma = t_y + u_{yy} \zeta_y^2$ are elastic constants.

The underlying rotational invariance of the tubule in the embedding space is responsible for two essential features of F_{el} . Firstly, it enforces a strict vanishing of the $(\partial_y \vec{h})^2$ tension-like term, with curvature $(\partial_y^2 \vec{h})$ as the lowest order harmonic term in the Goldstone tangent mode $\partial_y \vec{h}$. The result is highly anisotropic bulk elastic energy. Rotational invariance also ensures that nonlinear elasticity can only come in through powers of nonlinear strain tensor $E(u, \vec{h}) \equiv \partial_y u + \frac{1}{2} (\partial_y \vec{h})^2$, and that this property must be preserved upon renormalization.

2.5.1. Anomalous elasticity of the tubule phase

Within harmonic approximation tubule, *bulk* rms transverse height undulations are given by

$$\langle |\vec{h}(\mathbf{x})|^2 \rangle \approx \int_{q_{\perp} > L_{\perp}^{-1}} \frac{d^{D-1} q_{\perp} dq_y}{(2\pi)^D} \frac{1}{t q_{\perp}^2 + \kappa q_y^4} \propto L_{\perp}^{5/2-D}. \quad (25)$$

This suggests that for “phantom” tubules, the upper critical dimension $D_{uc} = 5/2$, contrasting with $D_{uc} = 4$ for the flat phase.^{7,8} This also implies that rms fluctuations of the tubule normals are given by

$$\langle |\delta n_y(\mathbf{x})|^2 \rangle \propto L_{\perp}^{3/2-D}. \quad (26)$$

Since this diverges in the infra-red $L_{\perp} \rightarrow \infty$ for $D \leq D_{lc} = 3/2$, this harmonic bulk mode analysis (ignoring anomalous elasticity and zero modes) suggests that the lower critical dimension D_{lc} below which the tubule is necessarily crumpled is given by $D_{lc} = 3/2$.

As for the flat phase, one needs to assess the role of elastic nonlinearities that appear in free energy F_{el} , Eq.24. One way to do this is to integrate out the phonon u (which, at long scales can be done exactly). This leads to the only remaining

nonlinearity in \vec{h}

$$F_{\text{anh}}[\vec{h}] = \frac{1}{4} \int d^{D-1}x dy (\partial_y \vec{h} \cdot \partial_y \vec{h}) V_h(\partial_y \vec{h} \cdot \partial_y \vec{h}), \quad (27)$$

with the Fourier transform of the kernel given by

$$V_h(\mathbf{q}) = \frac{g_y g_\perp q_\perp^2}{g_y q_y^2 + g_\perp q_\perp^2}. \quad (28)$$

Because of the $|\mathbf{q}|_\perp \approx q_y^2$ ($z = 1/2$) anisotropy of the bulk \vec{h} modes, $V_h(\mathbf{q})$ scales as $g_\perp q_\perp$ at long scales, and therefore is strongly irrelevant near the Gaussian fixed point as long as g_\perp is not renormalized (but see below). It is straightforward to verify to *all* orders in perturbation theory, that in a phantom tubule, there is no such renormalization of g_\perp .¹³

However, as asserted earlier, the *full* elasticity Eq.24, *before* u is integrated out, *is* anomalous, because $g_y(\mathbf{q})$ is driven to zero as $q_y \rightarrow 0$, according to

$$g_y(\mathbf{q}) = q_y^{\eta_u} S_g(q_y/q_\perp^z), \quad (29)$$

with $S_g(x)$ universal scaling function:

$$S_g(x) \propto \begin{cases} \text{constant}, & x \rightarrow \infty \\ x^{-\eta_u}, & x \rightarrow 0, \end{cases} \quad (30)$$

and exact exponents:

$$z = \frac{1}{2}, \quad \eta_u = 5 - 2D. \quad (31)$$

One simple way to see this is to note that rotational invariance enforces graphical corrections to preserve the form of the nonlinear strain tensor $E(u, \vec{h}) \equiv \partial_y u + \frac{1}{2}(\partial_y \vec{h})^2$. This leads to a relation between η_κ , η_u and the anisotropy exponent z

$$2\eta_\kappa + \eta_u = 4 - (D - 1)/z \quad (32)$$

which, together with the defining relation $z = 2/(4 - \eta_\kappa)$ reduces to

$$2\eta_u - (D - 5)\eta_\kappa = 10 - 4D, \quad (33)$$

and for $\eta_\kappa = 0$ gives z and η_u in Eq.31. This is supported by a detailed self-consistent one-loop perturbative calculation of $g_y(\mathbf{q})$ and by direct RG analysis.¹³

For *phantom* membranes with $D = 2$, $\eta_u = 1$ and $z = 1/2$, we find:

$$g_y(\mathbf{q}) \propto \begin{cases} q_y, & q_y \gg \sqrt{q_\perp} \\ \sqrt{q_\perp}, & q_y \ll \sqrt{q_\perp}. \end{cases} \quad (34)$$

This leads to phonon rms fluctuations given by

$$\langle u(\mathbf{x})^2 \rangle = L_\perp^{1/4} S_u(L_y/L_\perp^{3/4}), \quad (35)$$

with universal scaling function having limiting form

$$S_u(x) \propto \begin{cases} \text{constant}, & x \rightarrow \infty \\ x^{1/3}, & x \rightarrow 0. \end{cases} \quad (36)$$

For roughly square membranes, $L_y \sim L_\perp = L$, so, as $L \rightarrow \infty$, $L_y/L_\perp^{3/4} \rightarrow \infty$ this gives

$$\langle u(\mathbf{x})^2 \rangle = L_\perp^{1/4}, \quad (37)$$

a result that is consistent with simulations by Bowick, et al.⁴⁴

2.5.2. Zero-modes and tubule shape correlation

The tubule's shape is characterized by

$$R_G^2 \equiv \langle |\vec{h}(\mathbf{L}_\perp, y) - \vec{h}(0_\perp, y)|^2 \rangle, \quad h_{rms}^2 \equiv \langle |\vec{h}(\mathbf{x}_\perp, L_y) - \vec{h}(\mathbf{x}_\perp, 0)|^2 \rangle. \quad (38)$$

As illustrated in Fig.3 R_G measures the radius of a typical cross-section of the tubule perpendicular to its extended (y -) axis, and h_{rms} measures tubule end-to-end transverse fluctuations.

For a phantom tubule these are easily computed *exactly* using tubule free energy, Eq.24. One important subtlety is that one needs to take into account "zero modes" (Fourier modes with \mathbf{q}_\perp or $q_y = 0$), that, because of anisotropic scaling $q_\perp \sim q_y^2$ of the bulk modes can dominate tubule shape fluctuations.

For R_G one finds

$$R_G^2 = 2(d-D) \left[\frac{k_B T}{L_y} \int_{L_\perp^{-1}} \frac{d^{D-1} q_\perp}{(2\pi)^{D-1}} \frac{1}{t q_\perp^2} (1 - e^{i\mathbf{q}_\perp \cdot \mathbf{L}_\perp}) \right. \\ \left. + k_B T \int_{L_\perp^{-1}, L_y^{-1}} \frac{d^{D-1} q_\perp dq_y}{(2\pi)^D} \frac{(1 - e^{i\mathbf{q}_\perp \cdot \mathbf{L}_\perp})}{t q_\perp^2 + \kappa(\mathbf{q}) q_y^4} \right], \quad (39)$$

with the first and second terms coming from the $q_y = 0$ "zero mode" and the standard bulk contributions, respectively. From its definition, it is clear that the $\mathbf{q}_\perp = 0$ "zero mode" does not contribute to R_G . Standard asymptotic analysis of above integrals gives

$$R_G(L_\perp, L_y) = L_\perp^\nu S_R(L_y/L_\perp^z) \quad (40)$$

with, for phantom membranes,

$$\nu = \frac{5-2D}{4}, \quad z = \frac{1}{2}, \quad (41)$$

and the limiting form of the universal scaling function $S_R(x)$ given by

$$S_R(x) \propto \begin{cases} 1/\sqrt{x} & \text{for } x \rightarrow 0 \\ \text{constant,} & \text{for } x \rightarrow \infty. \end{cases} \quad (42)$$

This gives

$$R_G \propto L_\perp^\nu \propto L_\perp^{1/4}, \quad \text{for } D = 2, \quad (43)$$

for the physically relevant case of a square membrane $L_\perp \sim L_y \sim L \rightarrow \infty$, for which $L_y \gg L_\perp^z$, with bulk mode contribution dominating over the $q_y = 0$ zero mode. This result is in excellent quantitative agreement with simulations of Bowick,

et al.⁴⁴ who found $\nu = 0.24 \pm 0.02$, in $D = 2$. It would be interesting to test the full anisotropic scaling prediction of Eqs.40,42 by varying the aspect ratio of the membrane in such simulations. For instance, for fixed L_\perp and increasing L_y these predict *no* change in R_G . The same should hold if L_y is *decreased* at fixed L_\perp : R_G should remain unchanged until $L_y \sim \sqrt{L_\perp}$, at which point the tubule should begin to get thinner (i.e. R_G should decrease).

Equations 40 and 42 also correctly recover the limit of $L_y = \text{constant} \ll L_\perp^z \rightarrow \infty$, where the tubule simply becomes a phantom, coiled up, $D - 1$ -dimensional polymeric network of size L_\perp embedded in $d - 1$ dimensions, with the radius of gyration $R_G(L_\perp) \sim L_\perp^{(3-D)/2}$. In the physical dimensions ($D = 2$ and $d = 3$) this in particular gives a coiled up ideal polymer of length L_\perp with $R_G \sim L_\perp^{1/2}$, as expected.

Similar analysis for the tubule roughness h_{rms} gives

$$h_{rms}^2 = 2(d - D) \left[\frac{k_B T}{L_\perp^{D-1}} \int_{L_\perp^{-1}} \frac{dq_y}{(2\pi)} \frac{1}{\kappa(q_y) q_y^4} (1 - e^{iq_y L_y}) \right. \\ \left. + k_B T \int_{L_\perp^{-1}, L_y^{-1}} \frac{d^{D-1} q_\perp dq_y}{(2\pi)^D} \frac{(1 - e^{iq_y L_y})}{t q_\perp^2 + \kappa(\mathbf{q}) q_y^4} \right]. \quad (44)$$

In contrast to R_G , only the $\mathbf{q}_\perp = 0$ zero mode (first term) and bulk modes contribute to h_{rms} , giving

$$h_{rms}(L_\perp, L_y) = L_y^\zeta S_h(L_y/L_\perp^z) \quad (45)$$

with, for phantom membranes,

$$\zeta = \frac{5 - 2D}{2}, \quad z = \frac{1}{2}. \quad (46)$$

and the asymptotics of $S_h(x)$ given by

$$S_h(x) \propto \begin{cases} \text{constant} & \text{for } x \rightarrow 0 \\ x^{3/2-\zeta} & \text{for } x \rightarrow \infty \end{cases} \quad (47)$$

Equations 40 and 45 give information about the tubule roughness for arbitrarily large size L_\perp and L_y , and arbitrary aspect ratio. For the physically relevant case of a square membrane $L_\perp \sim L_y \sim L \rightarrow \infty$, for which $L_y \gg L_\perp^z$, in contrast to R_G (where bulk modes dominates), $\mathbf{q}_\perp = 0$ zero mode dominates, leading to

$$h_{rms} \propto \frac{L_y^{\zeta+(D-1)/2z}}{L_\perp^{(D-1)/2}} \propto L^{\zeta+(D-1)(1-z)/2z}, \quad (48)$$

Equations 18, 46 then give, for a $D = 2$ phantom tubule, $\zeta = 1/2$, $z = 1/2$

$$h_{rms} \sim \frac{L_y^{3/2}}{L_\perp^{1/2}}, \quad (49)$$

and therefore predicts for a square phantom membrane wild transverse tubule undulations

$$h_{rms} \sim L, \quad (50)$$

consistent with simulations⁴⁴ that find $h_{rms} \sim L^\gamma$, with $\gamma = 0.895 \pm 0.06$. As with R_G , it would be interesting to test the full scaling law Eq.45 by simulating non-square membranes, and testing for the independent scaling of h_{rms} with L_y and L_\perp . Note that, unlike R_G , according to Eq.49, h_{rms} will show immediate growth (reduction) when one increases (decreases) L_y at fixed L_\perp .

The above discussion also reveals that our earlier conclusions about the lower critical dimension D_{lc} for the existence of the tubule are strongly dependent on how L_\perp and L_y go to infinity relative to each other; i.e., on the membrane aspect ratio. The earlier conclusion that $D_{lc} = 3/2$ only strictly applies when the bulk modes dominate the physics, which is the case for a very squat membrane, with $L_y \approx L_\perp^z$, in which case $L_y \ll L_\perp$. For the physically more relevant case of a square *phantom* membrane, from the discussion above, we find that tubule phase is just marginally stable with $D_{lc} = 2^-$

Equations 40 and 45 also correctly recover the limit of $L_\perp^z = \text{constant} \ll L_y \rightarrow \infty$, where the tubule simply becomes a polymer (ribbon) of thickness $R_G(L_\perp)$ of length L_y embedded in $d - 1$ dimensions. These equations then correctly recover the polymer limit giving

$$h_{rms} \approx L_P(L_y/L_P)^{3/2}, \quad (51)$$

with L_\perp -dependent persistent length $L_P(L_\perp) \propto L_\perp^{D-1}$. So, as expected for a phantom tubule, if L_\perp does not grow fast enough (e.g. remains constant), while $L_y \rightarrow \infty$, the tubule behaves as a linear polymer and crumples along its axis and the distinction between the crumpled and tubule phases disappears.

2.6. Self-avoidance in the tubule phase

Self-avoidance is an important ingredient that must be included inside the tubule phase. Detailed analysis of self-avoidance overturns arguments in Sec.2.5.1, and leads to anomalous elasticity in the bending rigidity modulus $\kappa(\mathbf{q})$. Self-avoidance therefore also modifies the values of other shape exponents, while leaving the scaling form of correlation functions unchanged.

In the y-tubule phase the self-avoidance interaction F_{SA} from Eq.5 reduces to

$$F_{SA} = v \int dy d^{D-1} x_\perp d^{D-1} x'_\perp \delta^{(d-1)}(\vec{h}(\mathbf{x}_\perp, y) - \vec{h}(\mathbf{x}'_\perp, y)), \quad (52)$$

with $v = b/2\zeta_y$.

2.6.1. Flory theory

The effects of self-avoidance can be estimated by generalizing standard Flory arguments⁴⁵ from polymer physics⁴⁶ to the extended tubule geometry. The total self-avoidance energy scales as

$$E_{SA} \propto V \rho^2, \quad (53)$$

where $V \approx R_G^{d-1} L_y$ is the volume in the embedding space occupied by the tubule and $\rho = M/V$ is the embedding space density of the tubule. Using the fact that the tubule mass M scales like $L_\perp^{D-1} L_y$, we see that

$$E_{SA} \propto \frac{L_y L_\perp^{2(D-1)}}{R_G^{d-1}}, \quad (54)$$

Using the radius of gyration $R_G \propto L_\perp^\nu$, and considering, as required by the anisotropic scaling, a membrane with $L_\perp \propto L_y^2$, we find that $E_{SA} \propto L_y^{\lambda_{SA}}$ around the phantom fixed point, with

$$\lambda_{SA} = 1 + 4(D-1) - (d-1)\nu, \quad (55)$$

Self-avoidance is relevant when $\lambda_{SA} > 0$, which, from the above equation, happens for $\nu = \nu_{ph} = (5 - 2D)/4$ when the embedding dimension

$$d < d_{uc}^{SA} = \frac{6D-1}{5-2D}. \quad (56)$$

For $D = 2$ -dimensional membranes, $d_{uc}^{SA} = 11$. Thus, self-avoidance is strongly relevant for the tubule phase in $d = 3$, in contrast to the flat phase.

We can estimate the effect of the self-avoidance interactions on R_G in Flory theory, by balancing the estimate Eq.54 for the self-avoidance energy with a similar estimate for the elastic energy:

$$E_{elastic} = t \left(\frac{R_G}{L_\perp} \right)^2 L_\perp^{D-1} L_y. \quad (57)$$

Equating $E_{elastic}$ with E_{SA} , we obtain a Flory estimate for the radius of gyration R_G :

$$R_G(L_\perp) \propto L_\perp^{\nu_F}, \quad \nu_F = \frac{D+1}{d+1}, \quad (58)$$

which should be contrasted with the Flory estimate of $\nu_F^c = (D+2)/(d+2)$ for the *crumpled* phase. For the physical case $D = 2$, Eq.58 gives

$$R_G \propto L_\perp^{3/4}, \quad (59)$$

a result that is known to be *exact* for the radius of gyration of a $D = 1$ -polymer embedded in $d = 2$ -dimensions.⁴⁷ Since the cross-section of the $D = 2$ -tubule, crudely speaking, traces out a crumpled polymer embedded in two dimensions (see Fig.3), it is intriguing to conjecture that $\nu = 3/4$ is also the *exact* result for the scaling of the thickness of the tubule.

2.6.2. Renormalization group and scaling relations

A new significant complexity that arises and is special to the tubule phase (as compared to the crumpled phase) is the simultaneous presence of local elastic and nonlocal (in the intrinsic space) self-avoidance nonlinearities. Above Flory

mean-field analysis (that ignores elastic nonlinearities) is nicely complemented by a renormalization group approach that can handle this complexity of the full model $F = F_{el} + F_{SA}$, Eqs.24,52. Although, as we argued above, elastic nonlinearities are irrelevant in a phantom tubule, in a physical self-avoiding tubule, they are indeed important and lead to an anomalous bending rigidity elasticity.

The correct model, that incorporates the effects of both the self-avoiding interaction and the anharmonic elasticity, is defined by the full tubule free energy

$$F = \frac{1}{2} \int d^{D-1} x_{\perp} dy \left[\kappa (\partial_y^2 \vec{h})^2 + t (\partial_{\alpha}^{\perp} \vec{h})^2 + g_{\perp} (\partial_{\alpha}^{\perp} u)^2 + g_y \left(\partial_y u + \frac{1}{2} (\partial_y \vec{h})^2 \right)^2 \right] + v \int dy d^{D-1} x_{\perp} d^{D-1} x'_{\perp} \delta^{(d-1)}(\vec{h}(\mathbf{x}_{\perp}, y) - \vec{h}(\mathbf{x}'_{\perp}, y)) . \quad (60)$$

To assess the role of elastic (g_y) and self-avoiding (v) nonlinearities we implement standard momentum-shell RG.⁴⁸ We integrate out perturbatively in g_y and v short-scale fluctuations of modes $u(\mathbf{q})$ and $\vec{h}(\mathbf{q})$ within a cylindrical shell $\Lambda e^{-l} < q_{\perp} < \Lambda$, $-\infty < q_y < \infty$, and anisotropically rescale lengths (\mathbf{x}_{\perp}, y) and fields $(\vec{h}(\mathbf{x}), u(\mathbf{x}))$, so as to restore the ultraviolet cutoff to Λ :

$$\mathbf{x}_{\perp} = e^l \mathbf{x}'_{\perp} , \quad y = e^{z l} y' , \quad (61)$$

$$\vec{h}(\mathbf{x}) = e^{\nu l} \vec{h}'(\mathbf{x}') , \quad u(\mathbf{x}) = e^{(2\nu - z)l} u'(\mathbf{x}') , \quad (62)$$

where we have chosen the convenient (but not necessary) rescaling of the phonon field u so as to preserve the form of the rotation-invariant strain operator $\partial_y u + \frac{1}{2} (\partial_y \vec{h})^2$. Under this transformation the free energy returns back to its form, Eq.60, but with effective length-scale ($l = \log L_{\perp}$) dependent coupling constants determined by

$$\frac{dt}{dl} = [2\nu + z + D - 3 - f_t(v)]t , \quad (63)$$

$$\frac{d\kappa}{dl} = [2\nu - 3z + D - 1 + f_{\kappa}(g_y, g_{\perp})]\kappa , \quad (64)$$

$$\frac{dg_y}{dl} = [4\nu - 3z + D - 1 - f_g(g_y)]g_y , \quad (65)$$

$$\frac{dg_{\perp}}{dl} = [4\nu - z + D - 3]g_{\perp} , \quad (66)$$

$$\frac{dv}{dl} = [2D - 2 + z - (d - 1)\nu - f_v(v)]v , \quad (67)$$

where the various f -functions represent the graphical (i.e., perturbative) corrections. Since the self-avoiding interaction only involves \vec{h} , and (for convenience) the parameters in the \vec{h} propagator (t and κ) are going to be held fixed at 1, the graphical corrections coming from self-avoiding interaction alone depend only on the strength v of the self-avoiding interaction. Therefore, to *all* orders in v , and leading order in g_y , $f_t(v)$ and $f_v(v)$ are only functions of v and $f_{\kappa}(g_y, g_{\perp})$ and $f_g(g_y)$ are only functions of g_y and g_{\perp} .

It is important to note that g_{\perp} suffers no graphical corrections, i.e., Eq.66 is *exact*. This is enforced by an exact symmetry

$$u(\mathbf{x}_{\perp}, y) \rightarrow u(\mathbf{x}_{\perp}, y) + \chi(\mathbf{x}_{\perp}), \quad (68)$$

where $\chi(\mathbf{x}_{\perp})$ is an arbitrary function of \mathbf{x}_{\perp} , under which the nonlinearities in F are invariant.

We further note that there is an additional tubule “gauge”-like symmetry for $g_y = 0$

$$\vec{h}(\mathbf{x}_{\perp}, y) \rightarrow \vec{h}(\mathbf{x}_{\perp}, y) + \vec{\phi}(y), \quad (69)$$

under which the only remaining nonlinearity, the self-avoiding interaction, being local in y , is invariant. This “tubule gauge” symmetry demands that $f_{\kappa}(g_y = 0, g_{\perp}) = 0$, which implies that if $g_y = 0$, there is no divergent renormalization of κ , *exactly*, i.e., the self-avoiding interaction *alone* cannot renormalize κ . This *non*-renormalization of κ by the self-avoiding interaction, in a truncated (unphysical) membrane model with $g_y = 0$, has been verified to all orders in a perturbative renormalization group calculation.⁴⁹

To see that ν and z obtained as fixed point solutions of Eqs.63-67 have the same physical significance as the ν and z defined in the scaling expressions Eqs.1 for the radius of gyration R_G and tubule wigglyness h_{rms} , we use RG transformation to relate these quantities in the unrenormalized system to those in the renormalized one. This gives, for instance, for the radius of gyration

$$R_G(L_{\perp}, L_y; t, \kappa, \dots) = e^{\nu l} R_G(e^{-l} L_{\perp}, e^{-z l} L_y; t(l), \kappa(l), \dots), \quad (70)$$

Choosing $l = l_* = \log L_{\perp}$ this becomes:

$$R_G(L_{\perp}, L_y; t, \kappa, \dots) = L_{\perp}^{\nu} R_G(1, L_y/L_{\perp}^z; t(l_*), \kappa(l_*), \dots). \quad (71)$$

This relation holds for *any* choice of the (after all, arbitrary) rescaling exponents ν and z . However, *if* we make the special choice such that Eqs.63-67 lead to fixed points, $t(l_*)$, $\kappa(l_*)$, ... in Eq.71 go to *constants*, independent of l_* (and hence L_{\perp}), as L_{\perp} and hence l_* , go to infinity. Thus, in this limit, we obtain from Eq.71

$$R_G(L_{\perp}, L_y; t, \kappa, \dots) = L_{\perp}^{\nu} R_G(1, L_y/L_{\perp}^z; t_*, \kappa_*, \dots), \quad (72)$$

where t_* , κ_* , ... are the fixed point values of coupling constants. This result clearly agrees with the scaling forms for R_G , Eq.1 (with analogous derivation for h_{rms}) with the scaling function given by $S_R(x) \equiv R_G(1, x; t_*, \kappa_*, g_y^*, v^*)$.

The recursion relations Eqs.63-67 reproduce all of our earlier phantom membrane results (when $v = 0$, leading to $f_{\kappa} = 0$), as well as the upper-critical embedding dimension $d_{uc}^{SA} = (6D - 1)/(5 - 2D)$ for self-avoidance predicted by Flory theory, Eq.55, *and* the upper critical *intrinsic* dimension $D_{uc} = 5/2$ for anomalous elasticity for phantom membranes (determined by eigenvalues of dimensionless couplings corresponding to v and g_y). They also reproduce all of the Flory theory exponents

under the approximation that graphical corrections to t and v are the same, i.e., that $f_t(v_*) = f_v(v_*)$.

To analyze the renormalization of κ in a self-avoiding tubule, we focus once again on the nonlocal interaction the non-local interaction F_{anh} , Eq.27, mediated by integrated out phonons, with a kernel

$$V_h(\mathbf{q}) = \frac{g_y g_\perp q_\perp^2}{g_y q_y^2 + g_\perp q_\perp^2}, \quad (73)$$

whose long-scale scaling determines renormalization of κ . If $g_y(\mathbf{q})q_y^2 \gg g_\perp(\mathbf{q})q_\perp^2$ (as we saw for a phantom tubule) then at long scales $V_h(\mathbf{q}) \approx g_\perp q_\perp^2 / q_y^2 \sim q_y^2$ in the relevant limit of $q_\perp \sim q_y^2$. Simple power counting around the Gaussian fixed point then shows that this elastic nonlinearity is irrelevant for $D > D_{uc} = 3/2$, and therefore $f_\kappa^* = \eta_\kappa = 0$ for a physical $D = 2$ -dimensional tubule, as we argued in Sec.2.5.

On the other hand, if the scaling is such that $g_\perp(\mathbf{q})q_\perp^2$ dominates over $g_y(\mathbf{q})q_y^2$, then $V_h(\mathbf{q}) \approx g_y$, i.e. a constant at long length scales. Simple power-counting then shows that this coupling is relevant for $D < D_{uc} = 5/2$ and the bending rigidity modulus of a $D = 2$ -dimensional tubule is anomalous in this case.

In the RG language, the relevance of V_h is decided by the sign of the renormalization group flow eigenvalue of $g_\perp(l)$ in Eq.66

$$\lambda_{g_\perp} = 4\nu - z + D - 3, \quad (74)$$

which is exactly determined by the fixed-point values of ν and z , since g_\perp suffers no graphical renormalization.

As discussed in previous sections, for a phantom tubule (or for $d > d_{uc}$) $\nu = (5 - 2D)/4$ and $z = 1/2$. For d below but close to $d_{uc}^{SA} = (6D - 1)/(5 - 2D)$ ($= 11$ for $D = 2$), these values are modified by the self-avoiding interaction, but only by order $\epsilon \equiv d - d_{uc}^{SA}$. Hence a $D = 2$ -dimensional tubule, embedded in d dimensions close to $d_{uc}^{SA} = 11$, $\lambda_{g_\perp} \approx -1/2$ and $g_\perp(l)$ flows according to

$$\frac{dg_\perp}{dl} = [-\frac{1}{2} + O(\epsilon)]g_\perp, \quad (75)$$

i.e. g_\perp is *irrelevant* near $d = 11$ (for $\epsilon \ll 1$), $V_h(\mathbf{q}) \sim g_\perp q_\perp^2 / q_y^2 \sim q_y^{2-O(\epsilon)}$ is irrelevant to the *bend* elasticity for a $D = 2$ -dimensional tubule embedded in high dimensions near $d_{uc}^{SA} = 11$, and, hence, $f_\kappa = \eta_\kappa$ in Eq.64 vanishes as the fixed point. Therefore, in these high embedding dimensions the full model of a self-avoiding tubule reduces to the *linear* elastic truncated model with self-avoiding interaction as the only non-linearity, that can be nicely studied by standard expansion in $\epsilon = d_{uc}^{SA} - d$.⁴⁹ As we discussed above, the ‘‘tubule gauge’’ symmetry guarantees that in this case the self-avoiding interaction alone cannot renormalize κ , i.e., $f_\kappa = \eta_\kappa = 0$ for d near d_{uc}^{SA} . This together with Eq.64 at its fixed point leads to an *exact* exponent relation

$$z = \frac{1}{3}(2\nu + D - 1), \quad (76)$$

valid for a finite *range* $d_* < d < d_{uc}^{SA}$ of embedding dimensions, and for phantom tubules in any embedding dimension. Where valid, it therefore reduces the tubule problem to a single independent shape exponent.

However, this simple scenario, and, in particular, the scaling relation Eq.76, is *guaranteed* to break down as d is reduced. The reason for this is that, as d decreases, ν increases, and eventually becomes so large that the eigenvalue λ_{g_\perp} of g_\perp changes sign and becomes positive. As discussed earlier, once this happens, the nonlinear vertex Eq.73 becomes relevant, and κ acquires a divergent renormalization, i.e., $f_\kappa \neq 0$, and bend tubule elasticity becomes anomalous.

Now, it is easy to show, using Eq.76 and a rigorous lower bound $\nu > (D - 1)/(d - 1)$ inside λ_{g_\perp} , that it *must* become positive for $d > d_*^{lb}(D)$ with

$$d_*^{lb}(D) = \frac{4D - 1}{4 - D} = 7/2, \text{ for } D = 2. \quad (77)$$

Hence, for the case of interest $D = 2$ critical dimension d_* is bounded by $7/2$ from below. In fact, Flory and $\epsilon = 11 - d$ estimates indicate that $d_*(D = 2) \approx 6$.¹³

We therefore conclude that in a physical $D = 2$ -dimensional self-avoiding tubule, embedded in $d = 3 < d_* \approx 6$, anharmonic elasticity F_{anh} is important at long scales and leads to anomalous and divergent bending rigidity $\kappa(\mathbf{q})$ and $g_y(\mathbf{q})$

$$g_y(\mathbf{q}) = q_y^{\eta_u} S_g(q_y/q_\perp^z), \quad \kappa(\mathbf{q}) = q_y^{-\eta_\kappa} S_\kappa(q_y/q_\perp^z), \quad (78)$$

with

$$z\eta_\kappa = f_\kappa(g_y^*, g_\perp^*), \quad z\eta_u = f_g(g_y^*). \quad (79)$$

and asymptotic forms of scaling functions

$$S_g(x \rightarrow 0) \rightarrow x^{-\eta_u}, \quad S_\kappa(x \rightarrow 0) \rightarrow x^{\eta_\kappa}. \quad (80)$$

Another consequence is the breakdown of the exponent relation, Eq.76, that is replaced by *two* exact relations holding between *four* independent exponents z , ν , η_κ , and η_u

$$z = \frac{1}{3 - \eta_\kappa}(2\nu + D - 1), \quad z = \frac{1}{3 + \eta_u}(4\nu + D - 1), \quad (81)$$

which automatically contain the rotational symmetry Ward identity

$$2\eta_\kappa + \eta_u = 3 - (D - 1)/z, \quad (82)$$

formally arising from the requirement that graphical corrections do not change the form of the rotationally invariant strain operator $\partial_y u + \frac{1}{2}(\partial_y \vec{h})^2$. The existence of a nontrivial $d_* > 3$ and its consequences are summarized by Figs.6,7.

The physics behind above somewhat formal derivation of exponent relations (Ward identities) can be further exposed through a simple physical shell argument. As can be seen from Fig.8, bending of a tubule of radius R_G into an arc of radius R_c induces an in-plane strain energy density $g_y(L_y, L_\perp)(R_G(L_y)/R_c)^2$. Interpreting

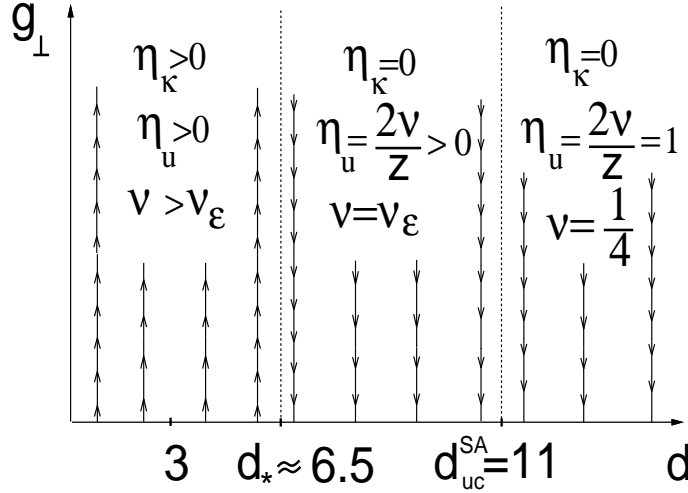


Fig. 6. Schematic illustration of change in relevance of $g_{\perp}(l)$ at d_* . For embedding dimensions below d_* (which includes the physical case of $d = 3$), $g_{\perp}(l)$ becomes relevant and (among other phenomena) leads to anomalous bending elasticity with $\kappa(\mathbf{q}) \sim q_y^{-\eta_{\kappa}}$, that diverges at long length scales.

this additional energy as an effective bending energy density $\kappa_y(L_{\perp}, L_y)/R_c^2$, leads to the *effective* bending modulus $\kappa_y(L_{\perp}, L_y)$,

$$\kappa_y(L_{\perp}, L_y) \sim g_y(L_{\perp}, L_y) R_G(L_{\perp}, L_y)^2. \quad (83)$$

This leads to a relation between the scaling exponents

$$2\nu = z(\eta_{\kappa} + \eta_u). \quad (84)$$

that is contained in Eqs.81 obtained through RG analysis above.

We note, finally, that all of the exponents must show a jump discontinuity at d_* . Therefore, unfortunately, an extrapolation from $\epsilon = 11 - d$ -expansion in a truncated model with linear elasticity⁴⁹ down to the physical dimension of $d = 3$ (which is rigorously below d_*) gives little information about the properties of a real tubule.

The computations for a physical tubule must be performed for $d < d_*$, where both the self-avoidance and the elastic nonlinearities are both relevant and must be handled simultaneously. As we discussed above, for $d < d_*$, the eigenvalue $\lambda_{g_{\perp}} > 0$, leading to the flow of $g_{\perp}(l)$ to infinity, which in turn leads to $V_h(\mathbf{q}) = g_y$. Physically this regime of $g_{\perp} \rightarrow \infty$ corresponds to freezing out the phonons u , i.e. setting $u = 0$ in the free energy $F[\vec{h}, u]$, Eq.60, with the resulting effective free energy functional for a physical self-avoiding tubule given by

$$F = \frac{1}{2} \int d^{D-1} x_{\perp} dy \left[\kappa (\partial_y^2 \vec{h})^2 + t (\partial_{\alpha}^{\perp} \vec{h})^2 + \frac{1}{4} g_y (\partial_y \vec{h})^4 \right] + v \int dy d^{D-1} x_{\perp} d^{D-1} x'_{\perp} \delta^{(d-1)}(\vec{h}(\mathbf{x}_{\perp}, y) - \vec{h}(\mathbf{x}'_{\perp}, y)), \quad (85)$$

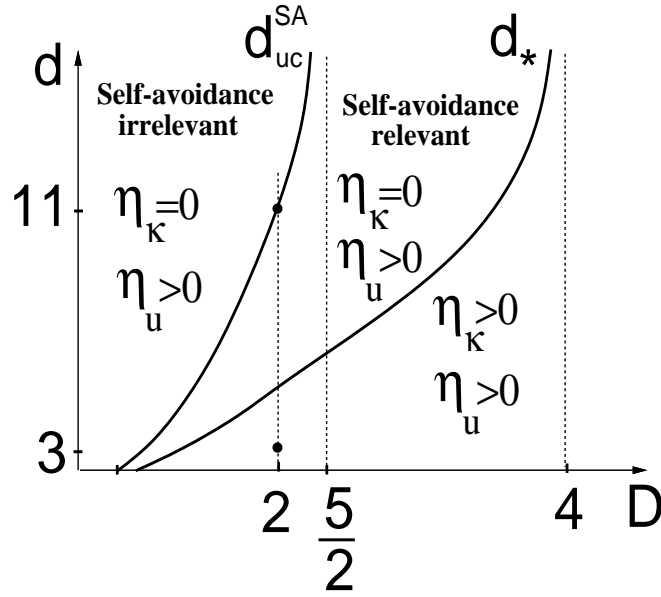


Fig. 7. Schematic of the tubule “phase” diagram in the embedding d vs intrinsic D dimensions. Self-avoiding interaction becomes relevant for $d < d_{uc}^{SA}(D) = (6D-1)/(5-2D)$, ($= 11$, for $D = 2$). Below the $d_*(D)$ curve (for which the lower bound is $d_*^l(D) = (4D-1)/(4-D)$) the anharmonic elasticity becomes relevant, leading to anomalous elasticity with a divergent bending rigidity.

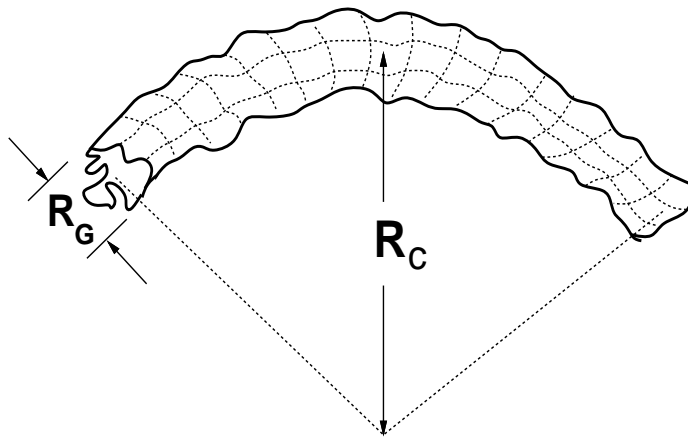


Fig. 8. Illustration of the physical mechanism for the enhancement of the bending rigidity κ by the shear g_y elasticity. To bend a polymerized tubule of thickness R_G into an arc of radius R_C requires R_G/R_C fraction of bond stretching and therefore costs elastic shear energy, which when interpreted as bending energy leads to a length-scale dependent renormalization of the bending rigidity κ and to the Ward identity Eq.84.

Since one must perturb in g_y around a nontrivial, *strong* coupling fixed point with $v^* = O(1)$, unfortunately, no controlled analysis of above model exists todate and remains a challenging open problem. Nevertheless, above RG analysis combined with Flory estimates and exact exponent relations provides considerable information about shape fluctuations and elasticity of a polymerized tubule.

2.7. Phase transitions

Now that we have solidly established the properties of the three phases of anisotropic polymerized membranes, we turn to analysis of phase transitions between them. As discussed in the Introduction, a direct crumpled-to-flat transition is highly non-generic for anisotropic membranes, as it has to be finely tuned to the tetracritical point illustrated in Fig.2. If so tuned this transition will be in the same universality class as for isotropic membranes (where it is generic).^{6,9}

Here we will focus on the new crumpled-to-tubule and tubule-to-flat transitions, which are generic for membranes with any amount of anisotropy. As for the tubule phase itself and the crumpled-to-flat transition, a complete analysis of these transitions must include both elastic and self-avoiding nonlinearities, a highly non-trivial open problem. Below we will instead present an incomplete solution. First we will present an RG analysis of a phantom (non-selfavoiding) membrane, focusing on the much simpler crumpled-to-tubule transition. We will then complement this study with a scaling theory and Flory approximation of the crumpled-to-tubule and tubule-to-flat transitions in a more realistic self-avoiding membrane.

2.7.1. Renormalization group analysis of crumpled-to-tubule transition

The crumpled-to-(y-)tubule (CT) transition takes place when $t_y \rightarrow 0$, while t_\perp remains positive. This implies that the CT critical point is characterized by highly anisotropic scaling $q_\perp \propto q_y^2$. It leads to a considerable simplification of the full free energy defined in Eq.5 down to

$$F[\vec{r}(\mathbf{x})] = \frac{1}{2} \int d^{D-1} x_\perp dy \left[\kappa_y (\partial_y^2 \vec{r})^2 + t_\perp (\partial_\alpha^\perp \vec{r})^2 + t_y (\partial_y \vec{r})^2 + \frac{u_{yy}}{2} (\partial_y \vec{r} \cdot \partial_y \vec{r})^2 \right]. \quad (86)$$

The standard $O(d)$ ϕ^4 model form of F facilitates systematic analysis using conventional RG methods.⁴⁸ Because of the strong *scaling* anisotropy of the quadratic pieces of the free energy, it is convenient to rescale lengths \mathbf{x}_\perp and y anisotropically:

$$\mathbf{x}_\perp = \mathbf{x}'_\perp e^l, \quad y = y' e^{zl}, \quad (87)$$

and rescale the “fields” $\vec{r}(\mathbf{x})$ according to

$$\vec{r}(\mathbf{x}) = e^{\chi l} \vec{r}'(\mathbf{x}'). \quad (88)$$

Under this transformation

$$\kappa_y(l) = \kappa_y e^{(D-1-3z+2\chi)l}, \quad t_\perp(l) = t_\perp e^{(D-3+z+2\chi)l}. \quad (89)$$

Requiring that both κ_y and t_\perp remain fixed under this rescaling (zeroth order RG transformation) fixes the “anisotropy” exponent z and the “roughness” exponent χ :

$$z = \frac{1}{2}, \quad \chi = (5/2 - D)/2. \quad (90)$$

Although this choice keeps the quadratic in \vec{r} part of F , Eq.86, unchanged, it *does* change the quartic piece:

$$u_{yy}(l) = u_{yy}e^{(D-1-3z+4\chi)l} = u_{yy}e^{(5/2-D)l}, \quad (91)$$

and shows that below the upper critical dimension $D_{uc} = 5/2$, the Gaussian critical point is unstable to elastic nonlinearities, that become comparable to harmonic elastic energies on scales longer than the characteristic length scale L_\perp^{nl}

$$L_\perp^{nl} = \left(\frac{\kappa_y}{u_{yy}} \right)^{1/(5/2-D)}. \quad (92)$$

To describe the new behavior that prevails on even *longer* length scales requires a full-blown RG treatment.

Such an analysis¹³ leads to corrections to the simple rescaling of κ_y , t_\perp , and t_y (due to u_{yy} non-linearity), characterized by “anomalous” exponents η_κ , η_t , and $\delta\theta$:

$$\kappa_y(l) = \kappa_y e^{(D-1-3z+z\eta_\kappa+2\chi)l}, \quad (93)$$

$$t_\perp(l) = t_\perp e^{(D-3+z+\eta_t+2\chi)l}, \quad (94)$$

$$t_y(l) = t_y e^{(D-1-z-\delta\theta+2\chi)l} \equiv t_y e^{\lambda_t l}, \quad (95)$$

that give

$$z = \frac{2 - \eta_t}{4 - \eta_\kappa}, \quad \chi = \frac{10 - 4D + \eta_\kappa(D - 3 + \eta_t) - 3\eta_t}{8 - 2\eta_\kappa},$$

valid at the new nontrivial CT critical point.

Once the values of η_t , η_κ and χ at the critical point are determined, the renormalization group gives a relation between correlation functions at or near criticality (small t_y) and at small wavenumbers (functions that are difficult to compute, because direct perturbation theory is divergent) to the same correlation functions away from criticality and at large wavenumbers (functions that can be accurately computed using perturbation theory). For example the behavior of the correlation lengths near the transition can be deduced in this way:

$$\xi_\perp(t_y) = e^l \xi_\perp(t_y e^{\lambda_t l}), \quad \xi_y(t_y) = e^{z l} \xi_y(t_y e^{\lambda_t l}), \quad (96)$$

assuming that a critical fixed point exists and all other coupling constants have well-defined values at this point. Taking $t_y e^{\lambda_t l} \approx 1$ then gives

$$\xi_\perp(t_y) \approx a t_y^{-\nu_\perp}, \quad \xi_y(t_y) \approx a t_y^{-\nu_y}, \quad (97)$$

where $a \approx \xi(1)$ is the microscopic cutoff and,

$$\nu_{\perp} = \frac{1}{\lambda_t} = \frac{4 - \eta_{\kappa}}{2(2 - \eta_t - 2\delta\theta) - \eta_{\kappa}(2 - \eta_t - \delta\theta)}, \quad \nu_y = z\nu_{\perp} \quad (98)$$

are correlation length exponents perpendicular and along the tubule axis.

The anomalous exponents can be computed by integrating out short-scale degrees of freedom perturbatively in u_{yy} . Standard analysis shows that indeed there is a nontrivial critical point (at a finite value of $u_{yy}^* = O(\epsilon)$, $\epsilon \equiv 5/2 - D$), at which, to all orders $\eta_t = 0$, and to one-loop order, for a physical membrane ($D = 2$, $d = 3$, i.e., $\epsilon = 1/2$)

$$\eta_{\kappa} = 0, \quad z = 1/2, \quad \chi = 1/4, \quad \nu_{\perp} \approx 1.227, \quad \nu_y \approx 0.614. \quad (99)$$

It is interesting to note that, in contrast to the treatment of crumpled-to-flat transition in isotropic membranes^{6,9}, where the critical point was only stable for an unphysically large value of the embedding dimension $d > 219$, the critical point characterizing the crumpled-to-tubule transition discussed here is stable for all d . Furthermore, the relatively small value of $\epsilon = 1/2$ (in contrast to for example $\epsilon = 2$ for flat phase and crumpling transition) gives some confidence that above critical exponents for the CT transition in a phantom membrane might even be quantitatively trustworthy.

2.7.2. Scaling theory of crumpled-to-tubule and tubule-to-flat transitions

Above RG analysis for the CT transition in phantom membranes, can be nicely complemented by a scaling theory combined with Flory estimates, that can incorporate both the elastic and self-avoiding nonlinearities, as we now describe.

Standard scaling arguments, supported by RG analysis and matching calculations (see e.g., Sec.2.5) suggest that near the crumpled-to-tubule transition, for a square membrane of internal size L , membrane extensions R_y and R_G along and orthogonal to the developing tubule axis should exhibit scaling form:

$$R_{G,y} = L^{\nu_{ct}^{G,y}} f_{G,y}(t_y L^{\phi}), \quad (100)$$

$$\propto \begin{cases} t_y^{\gamma_+^{G,y}} L^{\nu_c}, & t_y > 0, L \gg \xi_{ct} \\ L^{\nu_{ct}^{G,y}}, & L \ll \xi_{ct} \\ |t_y|^{\gamma_-^{G,y}} L^{\nu_t^{G,y}}, & t_y < 0, L \gg \xi_{ct} \end{cases}$$

where subscripts t , c and ct refer to tubule, crumpled and tubule-to-crumpled transition, respectively, and $\xi_{ct} \propto |t_y|^{-1/\phi}$ is a correlation length for the crumpled-to-tubule transition, $t_y = (T - T_{ct})/T_{ct}$, T_{ct} is the crumpled-to-tubule transition temperature, with $t_y > 0$ corresponding to the crumpled phase. Consistency demands that exponents $\gamma_{+/-}^{G,y}$ are given by

$$\gamma_+^{G,y} = \frac{\nu_c - \nu_{ct}^{G,y}}{\phi}, \quad \gamma_-^{G,y} = \frac{\nu_t^{G,y} - \nu_{ct}^{G,y}}{\phi}. \quad (101)$$

The asymptotic forms in Eq.100 are dictated by general defining properties of the phases and the CT transition. For example, scaling of both R_y and R_G like L^{ν_c} , with the same exponent ν_c in the crumpled phase is rooted in the isotropy of that phase. In contrast, extended and highly anisotropic nature of the tubule phase dictates that $\nu_t^G \neq \nu_t^y = 1$. The anisotropy is, however, manifested even in the crumpled phase through the different temperature-dependent amplitudes of R_G and R_y , with the aspect ratio R_y/R_G actually *diverging* as $T \rightarrow T_{ct}^+$, and membrane begins to extend into a tubule configuration. The former of these vanishes as $t_y \rightarrow 0^+$ (since the radius of gyration in the tubule phase is much less than that in the crumpled phase, since $\nu_t < \nu_c$), which implies $\gamma_+^G > 0$, while the latter diverges as $t_y \rightarrow 0^+$, since the tubule ultimately extends in that direction, which implies $\gamma_+^y < 0$.

We will now show how these general expectations are born out by the Flory theory. Following analysis very similar to that done in Sec.2.6.1, but keeping track of temperature-dependent order parameter ζ_y , we find that the Flory approximation to the free energy density in Eq.86, supplemented with self-avoidance is given by

$$f_{Fl}[R_G, \zeta_y] = t_y \zeta_y^2 + u_{yy} \zeta_y^4 + t_\perp \left(\frac{R_G}{L_\perp} \right)^2 + v \frac{L_\perp^{D-1}}{\zeta_y R_G^{d-1}}. \quad (102)$$

Minimizing this over R_G , gives

$$R_G \approx L_\perp^{\nu_t} \left(\frac{v}{t_\perp \zeta_y} \right)^{1/(d+1)}, \quad (103)$$

with the tubule exponent $\nu_t = \frac{D+1}{d+1}$ found earlier, but now with additional temperature and L_\perp dependence of R_G through $\zeta_y(t_y, L_\perp)$ that interpolates between tubule, crumpled and critical behavior. Inserting this expression for R_G into Eq.102, gives

$$f_{Fl}[\zeta_y] = t_y \zeta_y^2 + u_{yy} \zeta_y^4 + t_\perp^{\frac{d-1}{d+1}} \left(\frac{v}{\zeta_y} \right)^{\frac{2}{d+1}} L_\perp^{-\frac{2(d-D)}{d+1}}. \quad (104)$$

Minimizing $f_{Fl}[\zeta_y]$ in the crumpled phase ($t_y > 0$) gives

$$\zeta_y \approx \left(\frac{v^2 t_\perp^{d-1}}{t_y^{d+1}} \right)^{\frac{1}{2(d+2)}} L_\perp^{-\frac{d-D}{d+2}}, \quad (105)$$

that, as expected vanishes in the thermodynamic limit. For a square ($L \times L$) membrane this then gives for $R_y = \zeta_y L_y$ and R_G (using Eq.103)

$$R_y \propto t_y^{-\frac{d+1}{2(d+2)}} L_\perp^{\frac{D+2}{d+2}}, \quad R_G \propto t_y^{\frac{1}{2(d+2)}} L_\perp^{\frac{D+2}{d+2}}, \quad (106)$$

which, after comparing with the general form, Eq.100, gives

$$\nu_c = \frac{D+2}{d+2}, \quad \gamma_+^y = -\frac{d+1}{2(d+2)}, \quad \gamma_+^G = \frac{1}{2(d+2)}, \quad (107)$$

ν_c reassuringly agrees with the well-known Flory result for the radius of gyration exponent ν_c for a D -dimensional manifold, embedded in d dimensions,^{5,22,23,24} and $\gamma_+^{y,G}$ special to crumpled *anisotropic* membranes.

As anticipated earlier, $\gamma_+^y \neq \gamma_+^G$ implies that intrinsically anisotropic membrane are qualitatively distinct from isotropic ones even in the crumpled phase, as they exhibit a ratio of major to minor moment of inertia eigenvalues (related to R_G/R_y) that diverges as CT transition is approached.

Now for the tubule phase, characterized by $t_y < 0$ and a finite order parameter $\zeta_y > 0$, last term in f_{Fl} , Eq.104 is clearly negligible for $L_\perp > \xi_{cr}$ and simple minimization gives $\zeta_y \approx \sqrt{|t_y|/u_{yy}}$, which, when then inserting into $R_{y,G}$ and comparing with the general scaling forms gives for a square membrane

$$\nu_t^y = 1, \quad \gamma_-^y = \frac{1}{2}, \quad \nu_t^G = \frac{D+1}{d+1}, \quad \gamma_-^G = -\frac{1}{2(d+1)}. \quad (108)$$

Finally, right at the crumpled-to-tubule transition, $t_y = 0$, minimization of $f_{Fl}[\zeta_y]$ gives

$$\zeta_y \propto L_\perp^{-\frac{(d-D)}{3+2d}} \quad (109)$$

which, when inserted in $R_{y,G}$ gives the advertised critical scaling forms with exponents

$$\nu_{ct}^y = \frac{D+d+3}{2d+3}, \quad \nu_{ct}^G = \frac{2D+3}{2d+3}, \quad \phi = \frac{2(d-D)}{2d+3}. \quad (110)$$

that are reassuringly consistent with our independent calculations of exponents $\gamma_{+,-}^{G,y}$, ν_c , $\nu_{ct}^{G,y}$, and $\nu_{ct}^{y,y}$ using exact exponent relations above. For the physical case of a two dimensional membrane embedded in a three dimensions, ($D=2, d=3$)

$$\begin{aligned} \nu_c &= 4/5, \quad \nu_{ct}^G = 7/9, \quad \nu_{ct}^y = 8/9, \quad \nu_t = 3/4, \\ \gamma_+^G &= 1/10, \quad \gamma_+^y = -2/5, \quad \gamma_-^G = -1/8, \quad \gamma_-^y = 1/2, \quad \phi = 2/9, \end{aligned} \quad (111)$$

The singular parts of other thermodynamic variables obey scaling laws similar to that for $R_{G,y}$, Eq.100. For example, the singular part of the specific heat per particle $C_v \sim \frac{1}{L^D} \frac{\partial^2}{\partial t_y^2} (\frac{1}{2} t_y R_y^2 L^{D-2})$, using Eq.100 exhibits scaling form

$$\begin{aligned} C_v &= L^\beta g(t_y L^\phi), \\ &\propto \begin{cases} t_y^{-\alpha_+} L^{\beta-\alpha_+\phi}, & t_y > 0, L \gg \xi_{ct} \\ L^\beta, & L \ll \xi_{ct} \\ |t_y|^{-\alpha_-} L^{\beta-\alpha_-\phi}, & t_y < 0, L \gg \xi_{ct} \end{cases} \end{aligned} \quad (112)$$

with $g(x) \approx \frac{d^2}{dx^2} [f_y^2(x)]$, and

$$\beta = 2\nu_{ct}^y - 2 + \phi, \quad \alpha_\pm = -2\gamma_\pm^y + 1, \quad (113)$$

$$\beta = 0, \quad \alpha_+ = \frac{2d+3}{d+2}, \quad \alpha_- = 0, \quad \text{Flory theory.} \quad (114)$$

This leads to the unusual feature that outside the critical regime (i.e. for $L \gg \xi_{ct}$), the singular part of the specific heat above the crumpled-to-tubule transition vanishes in the thermodynamic limit like $L^{-\alpha+\phi} \sim L^{-2(d-D)/(d+2)} \sim L^{-2/5}$. Similar behavior was also found for the direct crumpled-to-flat transition by Paczuski et al.⁶

We now turn to the tubule-to-flat (TF) transition. On both sides of this transition, $R_y = L_y \times O(1)$. Therefore only R_G exhibits critical behavior, which can be summarized by the scaling law:

$$R_G = L^{\nu_{tf}^{\perp,y}} f^{\perp}(t_{\perp} L^{\phi_{tf}}),$$

$$\propto \begin{cases} t_{\perp}^{\gamma_{+}^{tf}} L^{\nu_{t}}, & t_{\perp} > 0, L \gg \xi_{tf} \\ L^{\nu_{tf}}, & L \ll \xi_{tf} \\ |t_{\perp}|^{\gamma_{-}^{tf}} L, & t_{\perp} < 0, L \gg \xi_{tf} \end{cases} \quad (115)$$

where $t_{\perp} = (T - T_{tf})/T_{tf}$, $t_{\perp} > 0$ corresponds to the tubule phase, $\xi_{tf} \propto |t_{\perp}|^{-1/\phi_{tf}}$ is the correlation length for this transition, and the exponents obey the scaling relations

$$\gamma_{+}^{tf} = (\nu_t - \nu_{tf})/\phi_{tf}, \quad \gamma_{-}^{tf} = (1 - \nu_{tf})/\phi_{tf}. \quad (116)$$

In Flory theory we find:

$$\phi_{tf} = 1/3, \quad \nu_{tf} = 5/6, \quad \gamma_{+}^{tf} = -1/4, \quad \gamma_{-}^{tf} = -1/2. \quad (117)$$

The singular part of the specific heat again obeys a scaling law:

$$C_v = L^{2\nu_{tf} + \phi_{tf} - 2} g(t_{\perp} L^{\phi_{tf}}),$$

$$\propto \begin{cases} t_{\perp}^{-\alpha_{+}^{tf}} L^{-\kappa_{+}}, & t_{\perp} > 0, L \gg \xi_{tf} \\ L^{2\nu_{tf} + \phi_{tf} - 2}, & L \ll \xi_{tf} \\ |t_{\perp}|^{-\alpha_{-}^{tf}} L^{-\kappa_{-}}, & t_{\perp} < 0, L \gg \xi_{tf} \end{cases} \quad (118)$$

where, in Flory theory,

$$\alpha_{+}^{tf} = 3/2, \quad \alpha_{-}^{tf} = 0, \quad \kappa_{+} = 1/2, \quad 2\nu_{tf} + \phi_{tf} - 2 = \kappa_{-} = 0. \quad (119)$$

Thus, again, the singular part of the specific heat vanishes (now like $L^{-1/2}$) in the thermodynamic limit above (i.e., on the tubule side of) the transition, while it is $O(1)$ and smooth as a function of temperature in both the critical regime and in the flat phase.

3. Random Heterogeneity in Polymerized Membranes

3.1. Motivation

Soon after a general picture of idealized homogeneous membranes was established, much of the attention turned to effects of random heterogeneity on conformational properties of polymerized membranes.⁵⁰ As with many other condensed matter

systems (e.g., random magnets, pinned charged density waves, vortex lattices in superconductors)⁵¹ a main motivation is that random inhomogeneity is an inevitable feature in most physical membrane realizations. As illustrated a cartoon of cellular membrane wall (Fig.1.4 in lectures by Stan Leibler), functional proteins, nanopores (controlling ionic flow through membrane), and other heterogeneities (with sincere apologies to biologists for such crude physicist’s terminology) are incorporated into a cellular lipid bilayer. Holes or tears, random variation in the local coordination number (disclinations), dislocations, grain-boundaries, and impurities incorporated into fishnet-like biopolymer spectrin network attached to cellular wall (as e.g., in red blood cells) are also substantial sources of inhomogeneity in membranes. Such defects in the two-dimensional polymer network are also inadvertently introduced during photo-polymerization of synthetic polymerized membranes. If one is only interested in statistical conformational properties of such membranes, these frozen-in heterogeneities can be treated as random quenched disorder, similar to treatment of impurities in other condensed matter contexts.⁵¹

Consistent with theoretical predictions⁵⁰, the fact that quenched internal disorder can drastically modify the conformational thermodynamics of polymerized membranes was first demonstrated experimentally by Mutz, Bensimon and Brienne⁵². They observed that partially (heterogeneous) polymerized vesicles undergo upon cooling a “wrinkling” transition to a folded rigid glassy structure that resembles a raisin. Natural interpretation of this important experiment as an evidence for a transition towards a crumpled spin-glass-like state provided strong motivation for further theoretical studies of quenched disorder in polymerized membranes.

Below we will describe a generalized model that includes effects of quenched disorder in a polymerized membrane and will show that (as in-plane anisotropy, discussed in previous section) it has drastic qualitative effects on long-length conformational properties of a polymerized membrane.

3.2. Model of a heterogeneous polymerized membrane

It is clear that above sources of heterogeneity lead to local random in-plane dilations and compressions and can therefore be modelled by local random stresses $-\sigma_{\alpha\beta}(\mathbf{x})u_{\alpha\beta}$. Geometrically this can be understood as a random preferred background metric $g_{\alpha\beta}^0(\mathbf{x}) = \delta_{\alpha\beta} + \eta_{\alpha\beta}^0(\mathbf{x})$ with strain $\tilde{u}_{\alpha\beta} = \frac{1}{2}(g_{\alpha\beta} - g_{\alpha\beta}^0(\mathbf{x}))$ measured relative to this deformed state, and metric $g_{\alpha\beta} = \partial_\alpha \vec{r} \cdot \partial_\beta \vec{r}$ seeking to relax to $g_{\alpha\beta}^0(\mathbf{x})$. These local in-plane stresses can and will be relaxed by buckling of the membrane into the third dimension that will tend to screen the elastic interaction, thereby lowering the elastic energy by partial trade-off between in-plane elastic energy and membrane bending (curvature κ) energy. However, as illustrated in Fig.9(a), because such randomness respects the reflection symmetry relating two sides of the membrane, the induced puckering will locally break this Ising symmetry *spontaneously*, and in a way specific to each configuration of disorder.

A qualitatively distinct form of quenched disorder that *explicitly* breaks reflection

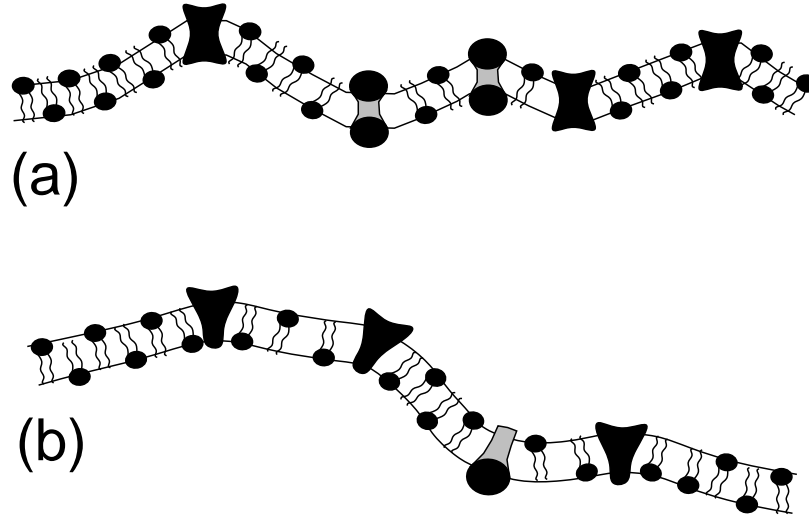


Fig. 9. A cartoon of a bilayer membrane with a reflection- (a) symmetric and (b) asymmetric inclusions that can be modelled by two qualitatively distinct types of disorder, the random stress and random mean curvature disorder, respectively

symmetry arises from asymmetric inclusions of the type illustrated in Fig.9(b). These lead to a local preferred extrinsic curvature, that, in the flat phase is described by $-\nabla^2 \vec{h} \cdot \vec{c}(\mathbf{x})$.

Membrane defects will also of course lead to heterogeneous elastic moduli, $\kappa(\mathbf{x})$, $\mu(\mathbf{x})$, and $\lambda(\mathbf{x})$. However, it can be shown that such weak heterogeneity (i.e., as long as the average value of these elastic constants remains larger than their variance, that is they are predominantly positive) has no qualitative effects on membrane long-scale conformations. Consequently, all effects of membrane heterogeneity can be modelled by just two types of quenched disorder, random stress and random curvature. This is perhaps not surprising given the aforementioned analogy of membranes with ferromagnet (with membrane normal \hat{n} playing the role of a spin \vec{S}), where too, random bond (that respects $\vec{S} \rightarrow -\vec{S}$) and random field (that is odd under $\vec{S} \rightarrow -\vec{S}$) are the only two qualitatively important types of quenched disorder. One qualitatively important distinction from random magnets that we can already anticipate at this point is that the curvature disorder, that couples to the gradient of the order parameter \hat{n} is far weaker perturbation than its ferromagnetic analog, the random field disorder that couples directly to magnetization. This distinction will lead to importance of the curvature disorder below $D_{uc} = 4$, (same as the random stress disorder and therefore competing with it) contrasting with the upper-critical dimension of $D_{uc} = 6$ of the random-field in a ferromagnet.⁵¹

The general model of heterogeneous membrane is therefore described by an

effective Hamiltonian $F[u_\alpha, \vec{h}]$

$$F[u_\alpha, \vec{h}] = \int d^D x \left[\frac{\kappa}{2} (\nabla^2 \vec{h} - \frac{\vec{c}(\mathbf{x})}{\kappa})^2 + \mu (u_{\alpha\beta})^2 + \frac{\lambda}{2} (u_{\alpha\alpha})^2 - \mu u_{\alpha\beta} \eta_{\alpha\beta}(\mathbf{x}) - \frac{\lambda}{2} u_{\beta\beta} \eta_{\alpha\alpha}(\mathbf{x}) \right], \quad (120)$$

where quenched disorder fields $\vec{c}(\mathbf{x})$ and $\eta_{\alpha\beta}(\mathbf{x})$ can be characterized by zero-mean, Gaussian statistics with second moment given by:

$$\begin{aligned} \overline{c_i(\mathbf{x})c_j(\mathbf{0})} &= \delta_{ij} \Delta_c(\mathbf{x}), \quad (121) \\ \overline{\eta_{\alpha\beta}(\mathbf{x})\eta_{\gamma\delta}(\mathbf{0})} &= (\Delta_1(\mathbf{x}) - \frac{1}{D} \Delta_2(\mathbf{x})) \delta_{\alpha\beta} \delta_{\gamma\delta} + \frac{1}{2} \Delta_2(\mathbf{x}) (\delta_{\alpha\gamma} \delta_{\beta\delta} + \delta_{\alpha\delta} \delta_{\beta\gamma}). \quad (122) \end{aligned}$$

Another useful form of this model is obtained after the phonons u_α are integrated out, which, at long length scales, can be done exactly since the phonons (unlike \vec{h}) are not soft and therefore can be approximated by a harmonic elasticity. The resulting Hamiltonian is given by

$$\begin{aligned} F[\vec{h}] &= \int d^D x \left[\frac{\kappa}{2} (\nabla^2 \vec{h} - \frac{\vec{c}(\mathbf{x})}{\kappa})^2 + \frac{1}{8} \partial_\alpha \vec{h} \cdot \partial_\beta \vec{h} \left\{ 2\mu P_{\alpha\gamma}^T P_{\beta\delta}^T + \frac{2\mu\lambda}{2\mu + \lambda} P_{\alpha\beta}^T P_{\gamma\delta}^T \right\} \partial_\gamma \vec{h} \cdot \partial_\delta \vec{h} \right. \\ &\quad \left. - \frac{1}{4} \eta_{\alpha\beta}(\mathbf{x}) \left\{ 2\mu P_{\alpha\gamma}^T P_{\beta\delta}^T + \frac{2\mu\lambda}{2\mu + \lambda} P_{\alpha\beta}^T P_{\gamma\delta}^T \right\} \partial_\gamma \vec{h} \cdot \partial_\delta \vec{h} \right] \quad (123) \end{aligned}$$

where $P_{\alpha\beta}^T = \delta_{\alpha\beta} - \frac{\partial_\alpha \partial_\beta}{\nabla^2}$ and $P_{\alpha\beta}^L = \frac{\partial_\alpha \partial_\beta}{\nabla^2}$ are transverse and longitudinal projection operators. For $D = 2, d = 3$ membrane $F[\vec{h}]$ simplifies considerably to:

$$F[\vec{h}] = \int d^2 x \left[\frac{\kappa}{2} (\nabla^2 h - \frac{c(\mathbf{x})}{\kappa})^2 + \frac{K}{8} (P_{\alpha\beta}^T \partial_\alpha h \partial_\beta h - P_{\alpha\beta}^T \eta_{\alpha\beta}(\mathbf{x}))^2 \right], \quad (124)$$

For a generic configuration of impurity disorder, the ground state is highly nontrivial as it is determined by simultaneous, but generically conflicting, minimization of the extrinsic and Gaussian curvature ($R = \frac{1}{2}((\nabla^2 h)^2 - (\partial_\alpha \partial_\beta h)^2)$) terms

$$\nabla^2 h = \frac{1}{\kappa} c(\mathbf{x}), \quad P_{\alpha\beta}^T \partial_\alpha h \partial_\beta h = P_{\alpha\beta}^T \eta_{\alpha\beta}(\mathbf{x}). \quad (125)$$

Long-scale properties of such ground state are amenable to statistical treatment, utilizing standard field theoretic machinery.

3.3. Weak quenched disorder: “flat-glass”

3.3.1. Short-range disorder

For many (but not all; see below) realizations of heterogeneity discussed above, such as for example random membrane inclusions, the disorder is short-ranged, and therefore can be characterized by δ -function correlated disorder with variances $\Delta_c(\mathbf{x}) = \Delta_c \delta^D(\mathbf{x})$, $\Delta_{1,2}(\mathbf{x}) = \Delta_{1,2} \delta^D(\mathbf{x})$.

To understand the effects of quenched disorder it is helpful to first study the stability of the flat phase (described by the anomalous elastic fixed point, studied in Sec.2.4) by performing a simple perturbative calculation in disorder and elastic

nonlinearities directly for a physical membrane ($D = 2, d = 3$). Standard analysis⁵⁰ then leads to disorder and thermally renormalized bending rigidity κ_R^D :

$$\begin{aligned} \kappa_R^D(q) = & \kappa + (k_B T \kappa + \Delta_c) \int \frac{d^2 p}{(2\pi)^2} \frac{K[\hat{q}_\alpha P_{\alpha\beta}^T(\mathbf{p})\hat{q}_\beta]^2}{\kappa^2 |\mathbf{q} + \mathbf{p}|^4} \\ & - (\Delta_1 + \Delta_2) \int \frac{d^2 p}{(2\pi)^2} \frac{K^2[\hat{q}_\alpha P_{\alpha\beta}^T(\mathbf{p})\hat{q}_\beta]^2}{4\kappa |\mathbf{q} + \mathbf{p}|^4}, \end{aligned} \quad (126)$$

The first, temperature-dependent correction that enhances κ is identical to that of a homogeneous membrane and is responsible for the stability of the flat phase of polymerized disorder-free membranes.³ At low temperature the temperature-independent contributions dominate. The last, random stress contribution leads to a divergent softening of the bending rigidity,⁵⁰ while the random curvature term works to increase the bending rigidity^{50,53}, and thereby works to stabilize the flat phase through the “order-from-disorder” mechanism that is the zero-temperature analog of the thermal one discussed in Sec.2.4.

Weak disorder should *not* affect the asymptotic behavior of membranes in the flat phase at sufficiently high temperatures, despite its importance at $T = 0$. To see this, assume the disorder is so weak that we can replace the elastic constants on the right hand side of Eq.126 by wave-vector-dependent quantities $\kappa_R(p)$ and $K_R(p)$ renormalized only by thermal fluctuations in the way controlled by the disorder-free flat phase fixed point. As discussed in Sec.2.4 these are expected to be singular at long scales, with $\kappa_R(p) \sim p^{-\eta_\kappa}$ and $K_R(p) \sim p^{\eta_u}$.^{3,7,8,9} The expression for $\kappa_R^D(q)$, Eq.126 becomes

$$\begin{aligned} \kappa_R^D(q) = & \kappa_R(q) + \Delta_c \int \frac{d^2 p}{(2\pi)^2} \frac{K_R(\mathbf{p})[\hat{q}_\alpha P_{\alpha\beta}^T(\mathbf{p})\hat{q}_\beta]^2}{\kappa_R^2(\mathbf{q} + \mathbf{p})|\mathbf{q} + \mathbf{p}|^4} \\ & - (\Delta_1 + \Delta_2) \int \frac{d^2 p}{(2\pi)^2} \frac{K_R^2(\mathbf{p})[\hat{q}_\alpha P_{\alpha\beta}^T(\mathbf{p})\hat{q}_\beta]^2}{4\kappa_R(\mathbf{q}|\mathbf{q} + \mathbf{p}|^4)}, \end{aligned} \quad (127)$$

$$= \kappa_R(q) [1 + \text{const.}\Delta_c q^{\eta_\kappa} - \text{const.}(\Delta_1 + \Delta_2)q^{\eta_u}], \quad (128)$$

where we made use of the exact 2D exponent relation^{3,7,8,9} $2\eta_f + \eta_u = 2$ (a consequence of rotational invariance). Since η_κ and η_u are positive, at finite temperature weak quenched disorder just gives a *subdominant* nonanalytic correction to disorder-free result for $\kappa_R(q)$. Physically this finite temperature irrelevance of disorder comes from singularly soft in-plane elastic moduli and divergent bending rigidity, that, respectively facilitate screening of the in-plane stress induced by impurities and suppress wrinkling effects of curvature disorder.

These perturbative arguments are supported by detailed renormalization group calculations controlled by an $\epsilon = 4 - D$ -expansion that show that at finite temperature the Aronovitz-Lubensky fixed point is stable to weak quenched disorder.⁵⁰ This is summarized by the RG flow equation of the coupling constants illustrated in Fig.10

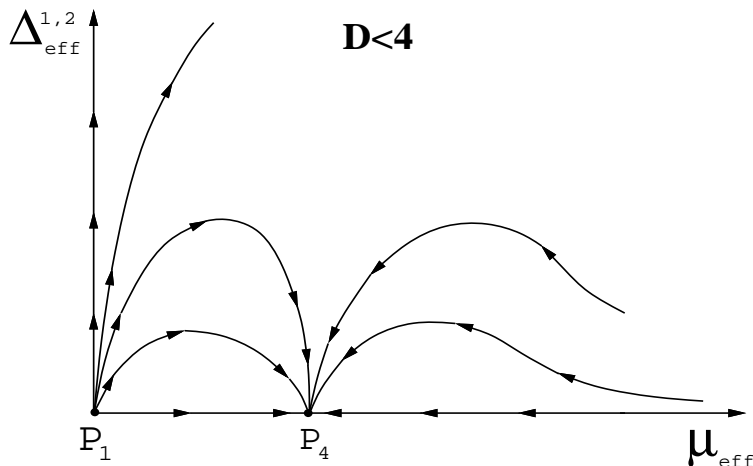


Fig. 10. RG flow diagram showing the irrelevance of random strain disorder (disorder variance scales to zero at long scales) near the disorder-free finite temperature fixed point P_4 controlling properties of the flat phase, and disorder induced instability of the flat phase at vanishing temperature ($\mu_{eff} \propto \mu T$).

However, as is clear from the flow diagram, for sufficiently low-temperatures, even weak bare strain disorder becomes strong (Δ 's flow to large values), invalidating above perturbative argument. In this case a full low temperature RG analysis is necessary. As first discovered by Morse, Lubensky and Grest, it shows^{9,50,53} that interplay of random stress and curvature disorder leads to a new stable zero-temperature fixed point that controls long-scale properties of the disorder-roughened polymerized membrane. Similar to the thermally rough flat phase described by the AL fixed point, the resulting $T = 0$ phase is characterized by a power-law roughness (with $\zeta < 1$) about on average flat configuration. It therefore has all the ingredients of the “flat-glass” phase anticipated by Nelson and Radzihovsky.⁵⁰

These RG results can be nicely complemented by the SCSA analysis.⁹ This can be done most effectively by first applying the replica formalism⁵⁴, that allows one to work with a translationally invariant effective Hamiltonian. To do this, one introduces n copies of fields \vec{h}^a and u_α^a labeled by the replica index a , and integrates out the quenched disorder, thereby obtaining a replicated Hamiltonian. Assuming commutability of the thermodynamic and the $n \rightarrow 0$ limits, the relation to the disorder-averaged free energy is established through the identity

$$\ln Z = \lim_{n \rightarrow 0} \frac{Z^n - 1}{n}, \quad (129)$$

where Z the partition function.

The membrane roughness is characterized by the full disorder-averaged height

correlation function (that can also be related to replicated ones):

$$\overline{\langle (\vec{h}(\mathbf{x}) - \vec{h}(\mathbf{0}))^2 \rangle} = \overline{\langle (\vec{h}(\mathbf{x}) - \vec{h}(\mathbf{0}))^2 \rangle}_{\text{conn}} + \overline{\langle \vec{h}(\mathbf{x}) - \vec{h}(\mathbf{0}) \rangle^2}, \quad (130)$$

$$\sim A_c |\mathbf{x}|^{2\zeta} + A |\mathbf{x}|^{2\zeta'}, \quad (131)$$

where, respectively, the first (connected) and second contributions characterize thermal- and disorder-generated roughness, with corresponding roughness exponents ζ and ζ' , and the overbar denotes configurational (disorder) averages. The related exponents characterizing the Fourier transform of these parts of the height correlation functions are given by $\zeta = (4 - D - \eta_\kappa)/2$ and $\zeta' = (4 - D - \eta'_\kappa)/2$. Analysis very similar to that done for homogeneous membranes in Sec.2.4.2, but with additional replica matrix structure leads to a zero-temperature fixed point, that is marginally unstable to finite temperature.⁵³ It is characterized by $\eta_\kappa = \eta'_\kappa$, with

$$\eta_\kappa(d_c, D) = \eta_\kappa^{\text{pure}}(4d_c, D), \quad (132)$$

where $\eta_\kappa^{\text{pure}}(d_c, D)$ is the SCSA exponent for η_κ found in Sec.2.4.2 characterizing a homogeneous polymerized membrane at a finite temperature. The underlying reasons for this amazing connection between roughness exponents at the disorder- and thermally-dominated fixed points is unclear. However, this SCSA prediction agrees with the $1/d_c$ - and ϵ -expansions to lowest order in respective small parameters. For a physical membrane, $D = 2$, $d_c = 1$, SCSA predicts:

$$\eta = 2/(2 + \sqrt{6}) = 0.449, \quad \zeta = 0.775, \quad (133)$$

that compares quite well (and much better than the lowest order ϵ - or $1/d_c$ -expansions) with the numerical simulation⁵³ result $\zeta = 0.81 \pm 0.03$ for a heterogeneous polymerized membrane.

3.3.2. Long-range disorder

Above analysis of short-range impurity disorder can be easily extended to treat disorder with long-range correlations, that can arise from weakly correlated distribution of frozen-in dislocations and disclinations, random grain boundaries⁵⁵, and from polymerized-in quasi-long-range correlated lipid tilt (or other membrane vector) order. At long scales, such disorder can be characterized by variances with power-law Fourier transforms:

$$\Delta_c(\mathbf{q}) = \Delta_c q^{-z_c}, \quad (134)$$

$$\Delta_{1,2}(\mathbf{q}) = \Delta_{1,2} q^{-z_{1,2}}, \quad (135)$$

where z_c and $z_{1,2}$ are curvature and stress disorder correlation exponents. Such long-range disorder considerably enriches the phase diagram of heterogeneous polymerized membranes, introducing a number of new flat-glass phases, that are summarized as function of value of these range exponents in Fig.11. For sufficiently short-ranged disorder (both z_c and $z_{1,2}$ small), and for finite and zero temperature,

we respectively recover the SCSA exponents for the Aronovitz-Lubensky^{7,8,9} and Morse-Lubensky^{53,9} fixed points.

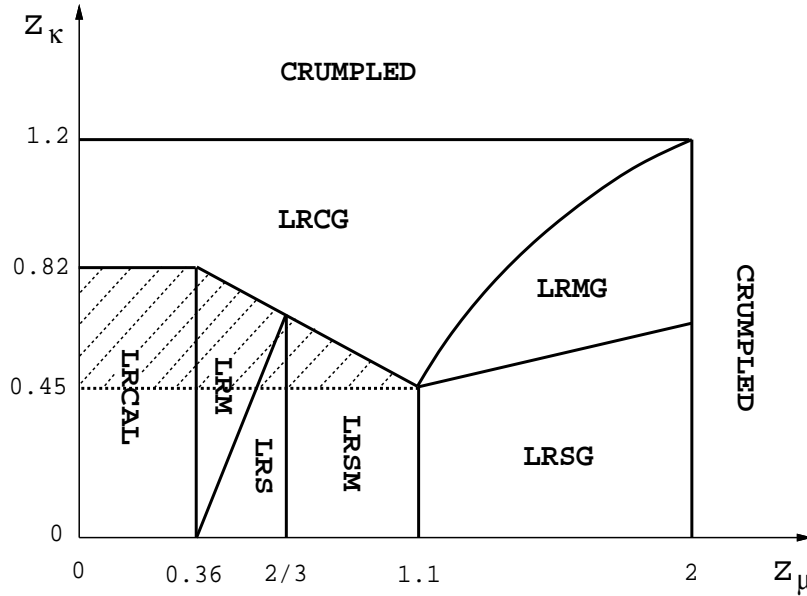


Fig. 11. Domain of stability of the flat phases as a function of z_μ, z_κ . (1) Disorder-dominated phases ($\zeta' > \zeta$): long-range stress glass (LRSG), long-range curvature glass (LRCG), long-range mixed glass (LRMG). (2) Temperature-dominated phases ($\zeta' < \zeta$): LR curvature (LRCAL), LR mixed (LRM) and LR stress (LRS). (3) LRSM: marginal phase with $\zeta = \zeta'$. The shaded area corresponds to a region of thermal phase transitions between several stable phases (LRCG and the others). The region where the membrane crumples is indicated.

More generally, the nature of the stable phases strongly depends on the value of the disorder-range z exponents and divides into three classes: (1) $\zeta > \zeta'$ with temperature dominated roughness, (2) $\zeta < \zeta'$ with disorder dominated roughness, and (3) $\zeta = \zeta'$ with equal scaling of the disorder and thermal contributions to the membrane roughness. Each one of these regions then further subdivides into distinct flat-glass phases depending on whether long-range curvature, stress, or both types of disorders are relevant. That is, in the presence of long-range disorder four new flat-glass phases, stable at finite temperature appear: (i) short-range (SR) curvature and long-range (LR) stress disorder (LRSG in Fig.11), (ii) LR curvature and SR stress disorder (LRCG), (iii) LR disorder in both curvature and stress disorder (LRMG), and (iv) zero curvature disorder and LR stress disorder (not represented in Fig.11). In addition to these flat-glass phases three corresponding temperature-dominated flat phases (LRS, LRCAL, LRM), and two phases for which $\zeta = \zeta'$ appear. In the shaded area in Fig.11 several of these phases are stable. Phase transition controlled by strength of disorder and/or temperature is therefore expected between them.

For sufficiently long range disorder correlations (large z 's), the dominant roughness exponent ζ' reaches 1, presumably indicating disorder-driven crumpling transition, and therefore breakdown of the weak-disorder expansion about (on average) flat phase. The expected energy-driven crumpling instability to a qualitatively distinct *isotropic* “crumpled-glass” state is a priori of entirely different nature than the entropy-driven crumpling transition predicted for phantom membranes.

3.4. Strong quenched disorder: “crumpled-glass”

Description of the strongly disordered crumpled-glass phase and the associated transition is significantly more complicated, because in addition to complexities of conventional spin-glasses, nonlocal self-avoiding interaction must be included. Such crumpled phase is characterized by a vanishing average tangent field $\overline{\langle \partial_\alpha r_i \rangle}$ (hence crumpled), but with a nonzero crumpled-glass order parameter $\overline{\langle \partial_\alpha r_i \rangle \langle \partial_\beta r_j \rangle}$ analogous to Edwards-Anderson spin-glass order parameter in disordered magnets.⁵¹ Some progress toward description of such crumpled-glass phase in phantom membranes was made by Radzihovsky and Le Doussal⁵⁶, by utilizing a $1/d$ -expansion.^{41,42,43}

In the limit of large embedding dimension, $d \rightarrow \infty$, the *homogeneous* membrane model can be solved exactly.⁸ In contrast, for a *disordered* membrane even in the $d \rightarrow \infty$ limit the exact solution of the crumpled-glass phase appears to be intractable. The difficulty arises from the tensor structure of the crumpled-glass order parameter, that leads to a problem of matrix field theory, a notoriously difficult problem. However, some progress can be made within an additional mean-field like approximation that ignores fluctuations in the tensor crumpled-glass order parameter. To simplify technical aspects of the presentation it is convenient to specialize to a purely scalar stress-only disorder, described by random Gaussian, zero-mean dilations and compressions in the locally preferred metric, $g_{\alpha\beta}^0(\mathbf{x}) = \delta_{\alpha\beta}(1 + \delta g^0(\mathbf{x}))$. A much more questionable (but technically necessary) approximation is omission of the self-avoiding interaction, that is undoubtedly important in the crumpled-glass phase.

Because of the isotropic nature of the crumpled-glass phase, the model must be formulated in terms of d -dimensional conformation vector $\vec{r}(\mathbf{x})$. The effective Hamiltonian is given by

$$F[\vec{r}] = d \int d^D x \left[\frac{\kappa}{2} |\nabla^2 \vec{r}|^2 + \frac{\mu}{4} (\partial_\alpha \vec{r} \cdot \partial_\beta \vec{r} - g_{\alpha\beta}^0(\mathbf{x}))^2 + \frac{\lambda}{8} (\partial_\alpha \vec{r} \cdot \partial_\alpha \vec{r} - g_{\alpha\alpha}^0(\mathbf{x}))^2 \right] \quad (136)$$

where the elastic moduli were rescaled by d so as to obtain sensible and nontrivial results in the limit $d \rightarrow \infty$. Replicating F allows averaging over quenched disorder.⁵⁴ Then, introducing two Hubbard-Stratanovich fields $\chi_{\alpha\beta}$ and $Q_{ab\alpha\beta}^{ij}$ to decouple replica diagonal and off-diagonal nonlinearities, respectively, leads to an effective Hamiltonian that is quadratic in \vec{r} . This allows formal integration over \vec{r} , that is conveniently done around background configuration \vec{r}_0 . Now, ignoring fluctuations

in the Hubbard-Stratanovich fields, the values of the order parameters $\partial_\alpha \vec{r}_0$ and $Q_{ab\alpha\beta ij}^o$ are determined by minimizing the resulting replicated free energy, together with the equation of constraint relating $\chi_{\alpha\beta}$ to these order parameters.

Assuming that the replica symmetry breaking does not occur until higher order in $1/d$, as it happens in the random anisotropy axis model^{57,58} we look for the saddle point replica-symmetric solution of the following form,

$$\vec{r}_\alpha^o = \zeta x_\alpha \hat{e}_\alpha, \quad \chi_{\alpha\beta}^o = \chi \delta_{\alpha\beta}, \quad Q_{ab\alpha\beta ij}^o = Q \delta_{\alpha\beta} \delta_{ij} (1 - \delta_{ab}). \quad (137)$$

The corresponding saddle-point equations for ζ , χ and Q are given by:

$$(1 - \zeta^2) + 2\chi(\alpha + \beta D) = \frac{T}{2D} \int_0^\Lambda \frac{d^D k}{(2\pi)^D} \left[\frac{2}{\kappa k^2 + \chi + \frac{\hat{\Delta}}{2T} Q} + \frac{\hat{\Delta} Q/T}{(\kappa k^2 + \chi + \frac{\hat{\Delta}}{2T} Q)^2} \right], \quad (138)$$

$$\zeta^2 = Q \left(1 - \frac{\hat{\Delta}}{2D} \int_0^\Lambda \frac{d^D k}{(2\pi)^D} \frac{1}{(\kappa k^2 + \chi + \frac{\hat{\Delta}}{2T} Q)^2} \right), \quad (139)$$

$$\left(\chi + \frac{Q \hat{\Delta}}{2T} \right) \zeta = 0, \quad (140)$$

where Δ is scalar stress disorder variance and $\hat{\Delta} = (2\mu + D\lambda)\Delta$. For the special case of homogeneous membranes, $\Delta = 0$, these equations reassuringly reduce to those found by David, et al.⁸ and describe the crumpled-to-flat transition exactly to leading order in $1/d$.

For a heterogeneous membrane ($\hat{\Delta} > 0$) there are three distinct solutions to these saddle-point equations, corresponding to three different possibilities for the values of the pair of order parameters ζ and Q .

$$\zeta = 0, \quad Q = 0, \quad (141)$$

$$\zeta \neq 0, \quad Q \neq 0, \quad (142)$$

$$\zeta = 0, \quad Q \neq 0. \quad (143)$$

that correspond to the crumpled phase, flat phase and crumpled-glass phase of the membrane, respectively.

Critical properties of these three phases and phase boundaries between them can be obtained from a straightforward analysis of Eqs.138-140.⁵⁶ The phase behavior is summarized in Fig.12, illustrating that within this approximation the lower-critical dimension for the flat phase in the presence of quenched disorder is $D_{lc}^\Delta = 4$, and therefore for this model (in $d \rightarrow \infty$ limit) only crumpled-glass and thermal crumpled phases survive in $D = 2$ membranes.

For the flat phase saddle point equations give

$$\zeta^2 = A \left(1 - \frac{T}{T_c} \right) \left(1 - \frac{\Delta}{\Delta_c} \right), \quad Q = A \left(1 - \frac{T}{T_c} \right). \quad (144)$$

where critical crumpling transition temperature T_c and critical value of disorder Δ_c (not to be confused with the variance of the curvature disorder from Secs.3.2-3.3.2),

defining the rectangular boundaries of the flat phase, are given by

$$T_c^{-1} = \frac{1}{D} \int_0^\Lambda \frac{d^D k}{(2\pi)^D} \frac{1}{\kappa k^2}, \quad \Delta_c^{-1} = \frac{1}{2D} \int_0^\Lambda \frac{d^D k}{(2\pi)^D} \frac{1}{\kappa^2 k^4}, \quad (145)$$

and $A^{-1} = 1 + (\alpha + D\beta)\hat{\Delta}/T$. The power-law vanishing of these order parameters according $\zeta \sim (T_c - T)^{\beta_\zeta}$, $\zeta \sim (\hat{\Delta}_c - \hat{\Delta})^{\beta_\zeta}$ and $Q \sim (T_c - T)^{\beta_Q}$, defines the corresponding β exponents: $\beta_T^\zeta = 1/2$, $\beta_\Delta^\zeta = 1/2$, $\beta_T^Q = 1$.

Outside this rectangular region ζ vanishes and the membrane undergoes a crumpling transition out of the flat phase. For $\hat{\Delta} \leq \hat{\Delta}_c$ and as $T \rightarrow T_c$ the transition is to the crumpled phase, while for $T \leq T_c$ and as $\hat{\Delta} \rightarrow \hat{\Delta}_c$ flat phase is unstable to the crumpled-glass phase.

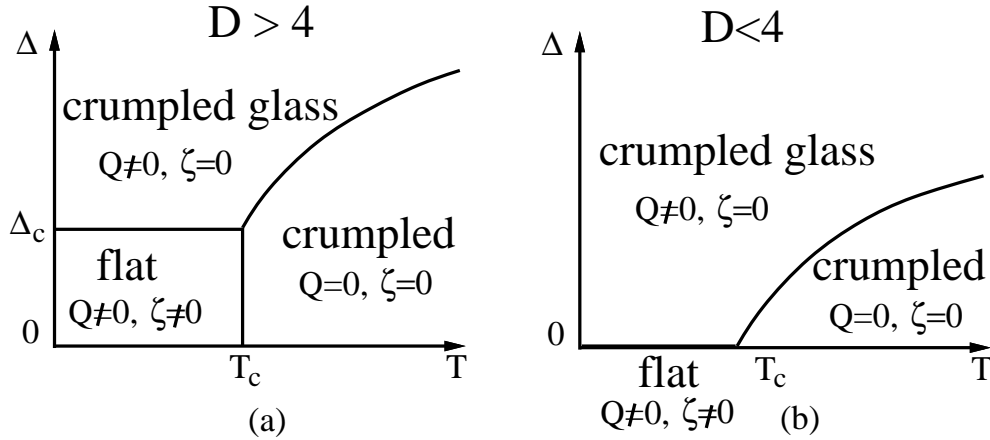


Fig. 12. A phase diagram for a disordered polymerized membrane showing (a) crumpled, flat-and crumpled-glass phases for $D > 4$. (b) In the physical case $D = 2 < 4$ the flat phase does not appear in this $d \rightarrow \infty$ limit, but is expected to when $1/d$ corrections are taken into account.

The glass susceptibility near the transition from the flat phase to the crumpled-glass phase can also be easily calculated by introducing an external field $h_{ij\alpha\beta} = h\delta_{ij}\delta_{\alpha\beta}$ conjugate to the crumpled-glass order parameter $Q_{ab\alpha\beta ij}$. The resulting saddle-point equations then lead to the crumpled-glass susceptibility, $\chi_{sg} = \partial Q/\partial h \sim (\hat{\Delta}_c - \hat{\Delta})^{-\gamma_{sg2}}$, with $\gamma_{sg2} = 1$.

Similarly, upon approach to the flat phase from the crumpled-glass (characterized by $Q \neq 0$ and $\zeta = 0$) the tangent susceptibility χ_ζ diverges as tangent order ζ spontaneously develops. Turning on an external field f that couples to the tangent order parameter, leads to $\chi_\zeta = \partial\zeta/\partial f \sim (\Delta - \Delta_c)^{-\gamma_{\zeta2}}$ giving $\gamma_{\zeta2} = 2/|4 - D|$, that, as expected diverges at the lower-critical dimension $D_c^\Delta = 4$ of the flat phase.

Finally, we look at the transition between the crumpled and crumpled-glass phases. The crumpled-glass susceptibility χ_{sg} near this transition is given by $\chi_{sg} \sim (\Delta_c(T) - \Delta)^{-\gamma_{sg1}}$, with $\gamma_{sg1} = 1$, as at the flat-to-crumpled-glass transition, except

for the modified phase boundary that is nonzero for any D :

$$\Delta_c^{-1}(T) = \frac{1}{2D} \int_0^\Lambda \frac{d^D k}{(2\pi)^D} \frac{1}{(\kappa k^2 + \chi(T))^2}, \quad (146)$$

and together with saddle-point equations and $Q = 0$, also defines the phase boundary between the crumpled and crumpled-glass phases for $D > 2$, $\Delta_c(T) - \Delta_c \sim (T - T_c)^\phi$, with ϕ the crossover exponent $\phi = |D - 4|/(D - 2)$.

As noted above, $d \rightarrow \infty$ analysis predicts an instability of the flat phase of $D = 2$ membranes to any amount of disorder ($D_{lc}^\Delta = 4$). A computation of $1/d$ corrections for the disordered membrane is technically quite challenging and remains an open problem. However, quite generally, anomalous elasticity generated by $1/d$ corrections (e.g., finite $\eta_\kappa = O(1/d)$ exponent⁸) strongly suggests the lowering of D_{lc}^Δ down to $D_{lc}^\Delta = 4 - O(1/d)$. This is supported by the Harris criterion applied to the buckling transition, controlled by the Aronovitz-Lubensky fixed point, that leads to stability of the flat phase (and the AL fixed point) as long as η_u remains positive. This is also consistent with the $\epsilon = 4 - D$ -expansion analysis of Radzihovsky and Nelson (performed for arbitrary d)⁵⁰, discussed in Sec.3.3.1, that the lower-critical dimension is reduced down to $D_{lc}^\Delta = 4 - 4/d$. A phase diagram for $D \leq 4$ consistent with the nature of the $1/d$ corrections is illustrated in Fig.13.

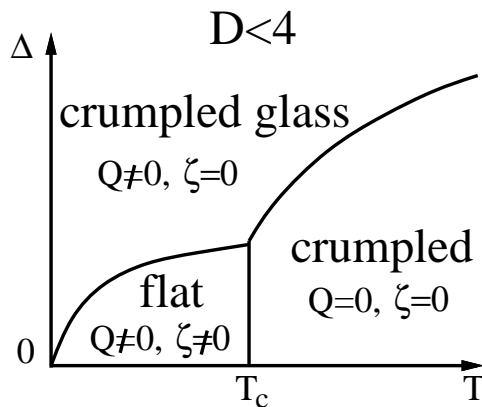


Fig. 13. Conjectured phase diagram for a disordered membrane $D \leq 4$ when $1/d$ corrections are taken into account, that allow a region of flat phase of size $1/d$ to appear.

Finally we observe that the crumpled-glass phase can be destroyed by applying an external tension to the membrane's boundaries. The metastable degenerate ground states would disappear and the average of the local tangents would no longer vanish. In this respect an external stress would be analogous to an external magnetic field in spin systems. As the stress is reduced the membrane would slowly return to the glassy phase but with some hysteresis. The line separating the regions of stable

and metastable degenerate states is then the analogue of the d'Almeida-Thouless line⁵⁹ studied in great detail for the real spin-glasses.⁵¹

4. Interplay of Anisotropy and Heterogeneity: Nematic Elastomer Membranes

We would like to conclude these lectures with a discussion of a new exciting realization of polymerized membranes, nematic elastomer membranes.¹¹ The motivation for their study is driven by recent experimental progress in the synthesis of nematic liquid-crystal elastomers¹², statistically isotropic and homogeneous gels of crosslinked polymers (rubber), with main- or side-chain mesogens, that can *spontaneously* develop nematic orientational order, accompanied by a spontaneous uniaxial distortion illustrated in Fig.14.

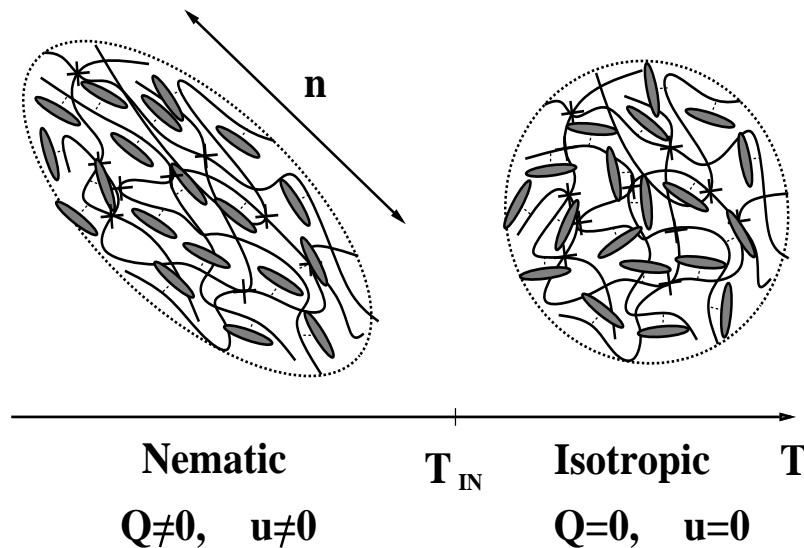


Fig. 14. Spontaneous uniaxial distortion of nematic elastomer driven by isotropic-nematic transition.

Even in the absence of fluctuations, *bulk* nematic elastomers were predicted³⁴ and later observed to display an array of fascinating phenomena^{12,35}, the most striking of which is the vanishing of stress for a range of strain, applied transversely to the spontaneous nematic direction. This striking softness is generic, stemming from the *spontaneous* orientational symmetry breaking by the nematic state^{34,35}, accompanied by a Goldstone mode⁶⁰, that leads to the observed soft distortion and strain-induced director reorientation⁶¹, illustrated in Fig.15. The hidden rotational symmetry also guarantees a vanishing of one of the five elastic constants³⁵, that usually characterize harmonic deformations of a three-dimensional uniaxial solid.²⁷ Given the discussion in Sec.2.4.1, not surprisingly, the resulting elastic softness leads

to qualitative importance of thermal fluctuations and local heterogeneity. Similar to their effects in smectic and columnar liquid crystals,^{30,31,32} thermal fluctuations lead to anomalous elasticity (universally length-scale dependent elastic moduli) in bulk homogeneous elastomers with dimensions below 3,^{36,37} and below 5, when effects of the random network heterogeneity are taken into account.³⁸

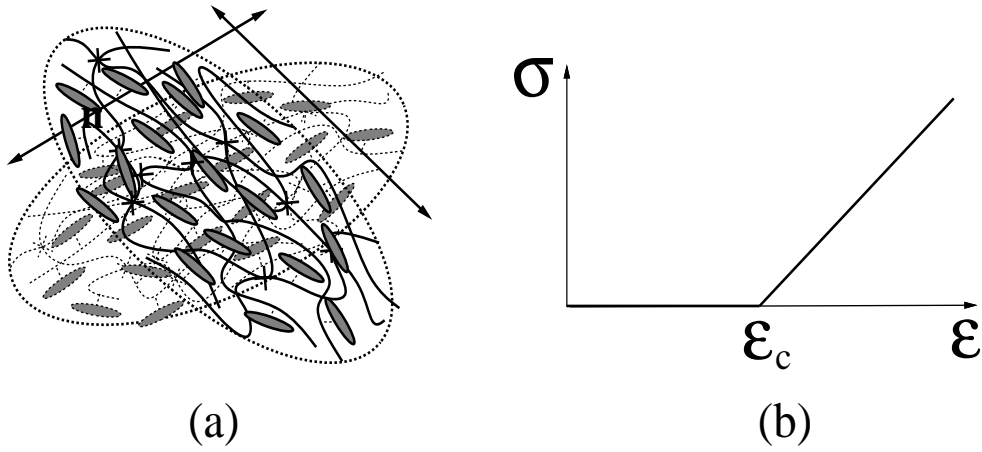


Fig. 15. (a) Simultaneous reorientation of the nematic director and of the uniaxial distortion is a low-energy nemato-elastic Goldstone mode of an ideal elastomer, that is responsible for its softness and (b) its flat (vanishing stress) stress-strain curve for a range of strains.

This rich behavior of bulk elastomers provided strong motivation to study nematic elastomer membranes (D -dimensional sheets of nematic elastomer fluctuating in d dimensions).¹¹ A model of such a membrane must incorporate both network anisotropy and heterogeneity discussed in previous sections. However, an important distinction from *explicitly* anisotropic membranes discussed in Sec.2 is that the nematic anisotropy is *spontaneously* chosen in the amorphous (initially statistically isotropic) elastomer matrix. At harmonic level this in-plane rotational symmetry can be captured by a two-dimensional harmonic effective Hamiltonian

$$\mathcal{H}_{NE}^0 = \frac{1}{2} \int d^2x [\kappa_{xx}(\partial_x^2 h)^2 + \kappa_{yy}(\partial_y^2 h)^2 + 2\kappa_{xy}(\partial_x^2 h)(\partial_y^2 h) + K_y(\partial_y^2 u_x)^2 + K_x(\partial_x^2 u_y)^2 + \lambda_x(\varepsilon_{xx})^2 + \lambda_y(\varepsilon_{yy})^2 + 2\lambda_{xy}\varepsilon_{xx}\varepsilon_{yy}], \quad (147)$$

with $\varepsilon_{\alpha\alpha} = \partial_\alpha u_\alpha$ (no sum over α implied here), and characterized by a uniaxial phonon elasticity with a vanishing transverse shear modulus, μ_{xy} . This latter feature is what distinguishes a nematic elastomer membrane from an *explicitly* anisotropic membrane discussed in Sec.2. The vanishing in-plane shear modulus captures at the harmonic level the invariance of the free energy under infinitesimal rotation of the nematic axis and the accompanying uniaxial distortion of the elastomer matrix. To ensure an in-plane stability curvature phonon elastic energies are included in \mathcal{H}_{NE}^0 .

As a result, in the putative flat nematic phase of an elastomer membrane, the phonons have qualitatively “softer” harmonic elasticity than in a conventional polymerized membrane discussed in Sec.2. Consequently, as in other “soft” systems (e.g., smectic and columnar liquid crystals phases; see discussion in Sec.2.4.1), in the presence of thermal fluctuations and/or heterogeneities, *nonlinear* elastic terms are essential for the correct description.

First principles derivation of the nematic elastomer model, that incorporates (hidden) in-plane rotational invariance at nonlinear level is somewhat involved and we refer an interested reader to recent detailed work on this subject.^{36,37} In short, one starts out with a model of a statistically homogeneous and isotropic elastic membrane coupled to a nematic in-plane order parameter $Q_{\alpha\beta}$. The rotational symmetry is then spontaneously broken by the nematic ordering at the isotropic-nematic transition, that also induces a spontaneous uniaxial in-plane distortion of the elastomer matrix, characterized by a strain tensor $u_{\alpha\beta}^0$. Expansion about this flat uniaxial state, ensuring underlying in-plane and embedding space rotational invariance leads to a nonlinear elastic Hamiltonian of a nematic elastomer membrane. Its form is that of the \mathcal{H}_{NE}^0 , Eq.147, but with the harmonic strain $\varepsilon_{\alpha\beta}$ replaced by a nonlinear strain tensor $w_{\alpha\beta}$, that incorporates both in-plane and height nonlinearities of the form $(\partial_x u_y)^2$ and $(\partial_x h)^2$, respectively.

In $D = 2$ both phonon and height anharmonic terms are strongly relevant (their perturbative corrections grow with length scale) and therefore must be both taken into account. One approach is to generalize the above model to a D -dimensional nematic elastomer membrane and perform an RG calculation controlled by an ϵ -expansion. However, it is easy to show that upper-critical dimensions for these nonlinearities are different, with height undulations becoming relevant below $D_{uc}^h = 4$, and smectic-like and columnar-like in-plane nonlinearities with upper-critical dimensions of $D_{uc}^{sm} = 3$ and $D_{uc}^{col} = 5/2$, respectively. Hence for $D > 3$, in-plane phonon nonlinearities can be neglected, with height undulation nonlinearities (of the type studied in Secs.2.4.2,2.5.1 the only remaining relevant ones for $D < 4$, and controllable close to $D = 4$ with an $\epsilon = 4 - D$ -expansion.

Generically, one would expect these undulation nonlinearities to renormalize bending rigidities $\kappa_{\alpha\beta}$ as well as in-plane elastic moduli $\lambda_{\alpha\beta}$, leading to anomalous elasticity with $\kappa_{\alpha\beta}(\mathbf{q}) \sim q^{-\eta_\kappa}$, $\lambda_{\alpha\beta}(\mathbf{q}) \sim q^{\eta_\lambda}$. As discussed in Sec.2.4.2, here too, rotational invariance imposes an exact Ward identity between exponents:

$$2\eta_\kappa + \eta_\lambda = \epsilon = 4 - D. \quad (148)$$

However, it is not difficult to show¹¹, that once in-plane nonlinearities are neglected (legitimate for $D > 3$), the harmonic phonons can be integrated out exactly, and lead to a purely harmonic effective Hamiltonian $\mathcal{H}[h]$. Therefore there is a strict *nonrenormalization* of the bending rigidity tensor $\kappa_{\alpha\beta}$ for $D > 3$. This together with the Ward identity, Eq.148 gives

$$\eta_\kappa = 0, \quad \eta_\lambda = 4 - D, \quad (149)$$

a result that is supported by a detailed renormalization group calculation.¹¹ This analysis also makes contact and recovers some of the results previously obtained in the studies of isotropic polymerized membranes. In particular, the previously seemingly unphysical, the so-called “connected fluid”⁷ is realized as a fixed point of a nematically-ordered elastomer membrane that is unstable to the globally stable nematic-elastomer fixed point.¹¹

Despite of some success, there are obvious limitations of above description, most notably in its application to the physical case of $D = 2$ elastomer membranes and inclusion of the (usually more dominant) local network heterogeneity. The first shortcoming primarily has to do with the neglect of in-plane elastic nonlinearities, which, near the Gaussian fixed point become relevant for $D < 3$. While it is very likely that the subdominance of these in-plane nonlinearities relative to the undulation ones will persist some amount *below* $D = 3$ ⁶², we expect that in the physical case of $D = 2$ all three nonlinearities need to be treated on equal footing. Carrying this out in a consistent treatment remains an open and challenging problem.

Secondly, elastomers are only statistically homogeneous and isotropic, exhibiting significant local heterogeneity in the polymer network. As we saw in Sec.3, such internal quenched disorder has rich qualitative effects in ordinary polymerized membranes. Furthermore, recent work by Xing and Radzihovsky has demonstrated,³⁸ that interplay between nonlinear elasticity and random strains and torques (due to network heterogeneity) leads to disorder controlled anomalous elasticity even in three-dimensional bulk nematic elastomers. Because nematic elastomer membranes are far softer than ordinary polymerized membranes and their bulk analogs, we expect network heterogeneity to have strong and rich effects in these systems. Considerable research remains to work out the resulting phenomenology.

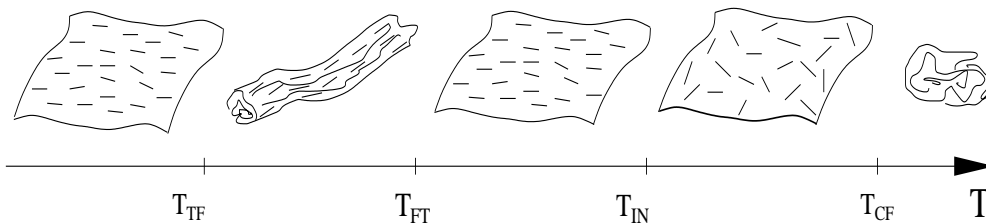


Fig. 16. A possible phase diagram for ideal nematic elastomer membranes. As the temperature is lowered a crumpled membrane undergoes a transition to isotropic flat phase at T_{CF} , followed by a 2D in-plane isotropic-nematic like transition to an anisotropic (nematic) flat phase. As T is lowered further, this anisotropic flat phase becomes unstable to a nematic tubule phase, where it continuously crumples in one direction but remains extended in the other. At even lower temperature, a tubule-flat transition takes place at T_{TF} .

It is interesting to conclude with a general discussion of the global conformational phase behavior of nematic elastomer membranes. As with ordinary polymerized membranes, upon cooling, isotropic elastomer membranes should undergo a

crumpling (flattening) transition from the crumpled to flat-isotropic phase. Upon further cooling, an in-plane (flat) isotropic-to-(flat) nematic transition can take place, leading to a flat membrane with a spontaneous in-plane nematic order. As for explicitly anisotropic membranes discussed in Sec.2, such nematically-ordered elastomer membranes should undergo further transition to a nematically-ordered tubule phase. Because of the in-plane rotation symmetry that is *spontaneously* (as opposed to explicitly) broken, such nematic tubule will exhibit in-plane elasticity (“soft” phonons) that is qualitatively distinct from tubules discussed in Sec.2.5.1, and will constitute a distinct phase of elastic membranes.⁶³ One interesting scenario of phase progression is the nematic-flat to nematic-tubule to nematic-flat reentrant phase transitions, driven by competition between growth of nematic order (anisotropy) and suppression of membrane’s out-of-plane undulations upon cooling, as schematically illustrated in Fig.16. Considerable research to elucidate the nature of the resulting fascinating phases and transitions remains.⁶³

5. Summary

In these notes, I have presented a small cross-section of the beauty and richness of fluctuating polymerized membranes. I have demonstrated the importance of the in-plane order in determining the long-scale conformations of these elastic sheets, by discussing in-plane anisotropy and local random heterogeneity and showed that these lead to a rich and highly nontrivial phenomenology.

6. Acknowledgments

The material presented in these lectures is an outcome of research done with a number of wonderful colleagues. The physics of anisotropic membranes presented in Section 1 is primarily based on extensive work done with John Toner. The Section 2 on heterogeneities in polymerized membranes is based on many years of fruitful collaboration with David Nelson and Pierre Le Doussal. And the final section is based on a collaboration with Xiangjun Xing, Tom Lubensky and Ranjan Mukhopadhyay. I am indebted to these colleagues for much of my insight into the material presented here. This work was supported by the National Science Foundation through grants DMR-0321848 and MRSEC DMR-0213918, the Lucile and David Packard Foundation and the A. P. Sloan Foundation.

References

1. L. Peliti and S. Leibler, *Phys. Rev. Lett.* **54**, 1690(1985); D. Foster, *Phys. Lett.* **A 114**, 115(1986); A. M. Polyakov, *Nucl. Phys.* **B 268**, 406(1986); F. David, *Europhys. Lett.* **2**, 577(1986).
2. F. David, E. Guitter, and L. Peliti, *J. Phys.***49**,2059(1987); E. Guitter and M.Kardar, *Europhys. Lett.* **13**, 441(1990). J. Park and T. C. Lubensky *Phys. Rev. E*, **53**, 2648 (1996).

3. D. R. Nelson and L. Peliti, *J. Phys. (Paris)* **48**, 1085(1987).
4. Crumpling, however, only takes place beyond an exponentially long persistence length $\xi_p = ae^{4\pi\kappa/3k_B T}$, that, in a typical liquid membrane at room temperature far exceeds its size, and therefore even a liquid membrane appears not crumpled.
5. Y. Kantor, M. Kardar and D. R. Nelson, *Phys. Rev. Lett.* **57**, 791(1986).
6. M. Paczuski, M. Kardar, and D. R. Nelson, *Phys. Rev. Lett.* **60**, 2638(1988).
7. J. A. Aronovitz and T. C. Lubensky, *Phys. Rev. Lett.* **60**, 2634 (1988); J. A. Aronovitz, L. Golubovic, and T. C. Lubensky, *J. Phys.(Paris)* **50**, 609(1989).
8. F. David and E. Guitter, *Europhys. Lett.* **5**, 709 (1988); E. Guitter, F. David, S. Leibler, and L. Peliti, *J. Phys. (Paris)* **50**, 1789 (1989).
9. P. Le Doussal and L. Radzihovsky, *Phys. Rev. Lett.* **69**, 1209 (1992). SCSA is incredibly successful in that for the flat phase of polymerized membranes it predicts exponents that are *exact* in $d \rightarrow \infty$, $d = D$ and correct to a leading order in $\epsilon = 4 - D$, thereby showing agreement with all known exact results on polymerized membranes. This approximation was introduced by Bray to treat ferromagnetic critical point in A. J. Bray, *Phys. Rev. Lett.* **32**, 1413 (1974).
10. D. Bensimon, private communication.
11. X. Xing, R. Mukhopadhyay, T. Lubensky, and L. Radzihovsky, *Phys. Rev. E* **68**, 021108 (2003).
12. M. Warner and E. M. Terentjev, *Prog. Polym. Sci.* **21**, 853(1996), and references therein; E. M. Terentjev, *J. Phys. Cond. Mat.* **11**, R239(1999).
13. L. Radzihovsky and J. Toner, *Phys. Rev. Lett.* **75**, 4752 (1995); *Phys. Rev. E* **57**, 1832 (1998).
14. We remind the reader here that this “tubule” phase is an anisotropic phase of *polymerized* membranes with a finite in-plane shear rigidity. This should not be confused with a similar, but distinct “tubule phase” observed in *liquid* lipid membranes studied in Refs.^{15,16,17}.
15. B. N. Thomas *et al.*, *Science* **267**, 1635 (1995).
16. C.-M. Chen, *Phys. Rev. E* **59**, 6192 (1999).
17. A. Rudolph, J. Calvert, P. Schoen, and J. Schnur, “Technological Developments of Lipid Based Tubule Microstructures”, in *Biotechnological Applications of lipid microstructures*, ed. B. Gaber *et al.* (Plenum, 1988); R. Lipkin, *Science*, **246**, 44 (December 1989).
18. Actually, in most current experimental realizations, the polymerization is random and leads to an isotropic membrane, making the isotropic case quite generic.
19. M. E. Fisher and D. R. Nelson, *Phys. Rev. Lett.*, **32**, 1350 (1974); D. R. Nelson, J. M. Kosterlitz, and M. E. Fisher, *Phys. Rev. Lett.*, **33**, 813 (1974), and *Phys. Rev. B* **13**, 412 (1976); A. Aharony, in *Phase Transitions and Critical Phenomena*, edited by C. Domb and M. S. Green (Academic, New York, 1976), Vol. 6, and *Bull. Am. Phys. Soc.* **20**, 16 (1975).
20. In these lectures we focus on the anisotropy in the membrane polymer network. This contrasts strongly with the anisotropy of the embedding space that membrane is fluctuating in. In this latter very interesting case considered in the work of Tokuyasu and Toner²¹ (with anisotropy introduced by application of an electric field), anisotropy has important qualitative effects even in the flat phase, where it lowers the lower-critical dimension for elastic nonlinearities down to $D_{uc} = 5/2$ and leads to a new anomalous elasticity fixed point with new universal exponents.
21. T. A. Tokuyasu and J. Toner, *Phys. Rev. Lett.* **68**, 3721 (1992).
22. M. Kardar and D. R. Nelson, *Phys. Rev. Lett.* **58**, 1289 (1987); **58**, 2280(E); *Phys. Rev. A* **38**, 966 (1988).

23. Y. Kantor and D. R. Nelson, *Phys. Rev. Lett.* **58**, 1289 (1987); Y. Kantor, M. Kardar, and D. R. Nelson, *Phys. Rev. A* **35**, 3056 (1987).
24. J. A. Aronovitz and T. C. Lubensky, *Europhys. Lett.* **4**, 395 (1987).
25. J. Toner, *Phys. Rev. Lett.* **62**, 905 (1988).
26. P. Hohenberg, *Phys. Rev.* **158**, 383 (1967); N. D. Mermin and H. Wagner, *Phys. Rev. Lett.* **17**, 1133 (1966); S. Coleman, *Commun. Math. Phys.* **31**, 259 (1973).
27. Landau and Lifshitz, *Theory of Elasticity*, Pergamon Press, (1975).
28. J. L. Cardy and S. Ostlund, *Phys. Rev. B* **25**, 6899 (1982); D.S. Fisher, *Phys. Rev. B* **31**, 7233 (1985); L. Radzihovsky and J. Toner, *Phys. Rev. B* **60**, 206 (1999).
29. For example, spin waves in a ferromagnetic state or antiferromagnetic state and phonons in an ordinary crystal (even in 2d), at long scales are faithfully described by a harmonic Hamiltonian, controlled by a Gaussian fixed point.
30. G. Grinstein and R. Pelcovits, *Phys. Rev. Lett.* **47**, 856 (1981); *Phys. Rev.* **A26**, 915 (1982).
31. L. Radzihovsky and J. Toner, *Phys. Rev. Lett.* **78**, 4414 (1997); *Phys. Rev. B* **60**, 206 (1999); B. Jacobsen, K. Saunders, L. Radzihovsky, and J. Toner, *Phys. Rev. Lett.* **83**, 1363 (1999).
32. K. Saunders, L. Radzihovsky, and J. Toner, *Phys. Rev. Lett.* **85**, 4309 (2000).
33. L. Radzihovsky, A. M. Ettouhami, K. Saunders, and J. Toner, *Phys. Rev. Lett.* **87**, 27001 (2001).
34. L. Golubovic and T. C. Lubensky, *Phys. Rev. Lett.* **63**, 1082 (1989).
35. T. C. Lubensky, R. Mukhopadhyay, L. Radzihovsky, X. Xing, *Phys. Rev. E* **66**, 011702 (2002).
36. X. Xing and L. Radzihovsky, *Europhys. Lett.* **61**, 769 (2003); University of Colorado preprint.
37. O. Stenull and T.C. Lubensky, *Europhys. Lett.* **61**, 779 (2003); cond-mat/030768.
38. X. Xing and L. Radzihovsky, *Phys. Rev. Lett.* **90**, 168301 (2003).
39. L. Radzihovsky and B. Jacobsen, unpublished.
40. M. Falcioni, M. Bowick, E. Gutter, and G. Thorleifsson, *Europhys. Lett.* **38**, 67 (1997).
41. S. Coleman, R. Jackiw and H. Politzer, *Phys. Rev. D* **10**, 2491 (1974); R. G. Root, *Phys. Rev. D* **10**, 3322 (1974).
42. This is analogous to the familiar $1/n$ expansion for critical phenomena, in which one expands about the number of spin components $n \rightarrow \infty$ limit.
43. Z. Justin, *Field Theory and Critical Phenomena*, Oxford Press (1994).
44. M. Bowick, M. Falcioni, and G. Thorleifsson, *Phys. Rev. Lett.* **79**, 885 (1997).
45. In the case of polymers, Flory theory agrees with the *exact* predictions for the radius of gyration exponent ν in *all* dimensions d where such exact predictions exist; in $d = 4, d = 2$, and $d = 1$, Flory theory recovers the exact results of $\nu = 1/2$, $\nu = 3/4$, and $\nu = 1$, respectively. And in $d = 3$ dimensions (where an exact result is not available) it agrees with the ϵ -expansion to better than 1%.
46. M. Doi and S. F. Edwards, *The Theory of Polymer Dynamics*, Oxford University, New York, 1986; P. G. de Gennes, *Scaling Concepts in Polymer Physics*, Cornell University, Ithaca, 1979.
47. B. Nienhuis, *Phys. Rev. Lett.* **49**, 1062 (1982); B. Duplantier in *Fields, Strings and Critical Phenomena*, Les Houches Lectures, edited by E. Brezin and J. Zinn-Justin (1990).
48. K. G. Wilson and J. Kogut, *Phys. Rep. C*, **12**, 77 (1977).
49. M. Bowick and E. Gutter, *Phys. Rev. E* **56** 7023 (1997).
50. L. Radzihovsky and D. R. Nelson, *Phys. Rev. A* **44**, 3525(1991); *Europhys. Lett.* **16**,

- 79 (1991).
51. K. Binder and A. P. Young, *Rev. Mod. Phys.*, **58**, 801 (1986); M. Chan, N. Mulders, and J. Reppy, *Physics Today* **30**, August (1996); D. S. Fisher, G. Grinstein, and A. Khurana, *Physics Today* **41**, December (1988); *Spin Glasses and Random Fields*, edited by A. P. Young, World Scientific, Singapore; T. Nattermann and S. Scheidl, *Advances in Physics* **49**, 607 (2000); *Liquid Crystals in Complex Geometries*, edited by G. P. Crawford and S. Žumer Taylor & Francis, London, (1996).
 52. M. Mutz, D. Bensimon, and M. J. Breinne, *Phys. Rev. Lett.* **67**, 923 (1991).
 53. D. Morse, T. C. Lubensky and G. S. Grest, *Phys. Rev. A* **45** R2151(1992); D. Morse and T.C. Lubensky, *Phys. Rev. A* **46**, 1751(1992).
 54. S. F. Edwards and P. W. Anderson, *J. Phys. (Paris)* **F 5**, 965 (1975).
 55. D. R. Nelson and L. Radzihovsky, *Phys. Rev. A* **46**, 7474 (1992).
 56. L. Radzihovsky and P. Le Doussal, *Journal de Physique I*, **2**, 599 (1991).
 57. Y. Y. Goldschmidt, *Phys. Rev. B* **30**, 1632 (1984).
 58. A. Khurana, A. Jagannathan, and J. M. Kosterlitz, *Nucl. Phys. B* **240**, [FS12] 1 (1984).
 59. J. R. d’Almeida and D. J. Thouless, *J. Phys. A* **64**, L743 (1989).
 60. We discuss here only “ideal” gels that exhibit a statistically isotropic and homogeneous high-temperature phase, in contrast to the so-called “semisoft” gels that are intrinsically anisotropic and therefore do not exhibit true nemato-elastic Goldstone mode.
 61. H. Finkelmann, I. Kundler, E.M. Terentjev, and M. Warner, *J. Phys. II* **7**, 1059(1997); G.C. Verwey, M. Warner, and E.M. Terentjev, *J. Phys. II (France)* **6**, 1273-1290(1996); M. Warner, *J. Mech. Phys. solids* **47**, 1355(1999).
 62. The situation is qualitatively similar to that of the ϕ^4 theory describing Ising transition. There too, the dominant nonlinearity is ϕ^4 that becomes relevant for $D < 4$, with the subdominant ϕ^6 nonlinearity near the Gaussian fixed point turning on only for $D \leq 3$. Despite of this one expects and indeed finds that ϕ^6 operator can be neglected even for $D = 3$ and $D = 2$, as the relevance analysis needs to be done near the interacting (Wilson-Fisher) and not near the Gaussian critical point. In the same way, we expect that subdominance of in-plane nonlinearities will survive even below $D = 3$, but probably not all the way down to the physical case of $D = 2$.
 63. X. Xing and L. Radzihovsky, unpublished.